Biomedicine & Pharmacotherapy 196 (2026) 119048

Contents lists available at ScienceDirect

Biomedicine & Pharmacotherapy

journal homepage: www.elsevier.com/locate/biopha

Involvement of Keap1/Nrf2 and the antioxidant defence in cytoprotective effects induced by cannabis polyphenols in SH-SY5Y neuronal cells

Guillermo Cásedas [a,b,*], Henar Rojas-Márquez [a,c,d], Lucía Ventura [a], Cristina Moliner [a], Filippo Maggi [e], Ainara Rubio-Castellanos [c,d,f,g], Víctor López [a,b,*]

[a] Department of Pharmacy, Faculty of Health Sciences, Universidad San Jorge, Villanueva de Gállego, Zaragoza 50830, Spain
[b] Instituto Agroalimentario de Aragón-IA2 (CITA-Universidad de Zaragoza), Zaragoza, Spain
[c] Departament of Genetics, Physical Anthropology and Animal Physiology, University of the Basque Country UPV/EHU, Leioa 48940, Spain
[d] Biobizkaia Health Research Institute, Cruces-Barakaldo 48903, Spain
[e] School of Pharmacy, University of Camerino, Camerino, Italy
[f] Ikerbasque, Basque Foundation for Science, Bilbao 48009, Spain
[g] CIBERDEM, Madrid 28029, Spain

ARTICLE INFO

Keywords:
SH-SY5Y
Oxidative stress
Cell signalling
Redox status
Antioxidant enzymes
Apoptosis

ABSTRACT

Oxidative stress (OS) is widely recognized as a central promoter to the pathogenesis of neurodegenerative diseases, including Alzheimer's disease (AD), Parkinson's disease (PD), amyotrophic lateral sclerosis (ALS) and primary lateral sclerosis (PLS). *Cannabis sativa* L. synthesizes a complex array of bioactive compounds that extends well beyond the well-known cannabinoids to include a diverse suite of polyphenols, terpenes, fatty acids, tocopherols, and proteins. The non-cannabinoid polyphenolic fraction is composed primarily of flavonoids, stilbenoids, lignans, and lignanamides, which contribute substantially to the plant's antioxidant, anti-inflammatory, and neuroprotective properties. This study investigates the redox-modulating and cytoprotective properties of a polyphenolic fraction derived from *Cannabis sativa L.* in SH-SY5Y neuroblastoma cells. Neurons were treated with various concentrations of the aqueous polyphenolic cannabis extract and exposed to oxidative stress using hydrogen peroxide (100 μM). Protein and gene expression related to redox signalling were analyzed via Western blot and qPCR, and molecular docking studies were performed *in silico*. Furthermore, antioxidant enzymes activity was measured by spectrophotometry. Results revealed that the phenolic fraction significantly activated the Keap1/Nrf2 pathway, increased expression of PRDX1 and PRDX3, and enhanced endogenous antioxidant defences. Simultaneously, it reduced endoplasmic reticulum stress-induced apoptosis (via Bax/Bcl-2 modulation) and attenuated inflammatory markers, including NO, NF-κB2, IL-6, and IL-8. *In silico* docking studies identified Leu583 as a key residue in Nrf2-ligand interactions. These findings suggest that *Cannabis sativa* L. polyphenols are key bioactive compounds modulating redox homeostasis and inflammation, and offering neuroprotective benefits with potential relevance in diseases involving mitochondrial dysfunction and oxidative damage.

1. Introduction

In the last decade, the study of the cannabis plant has increased exponentially. The understanding of cannabinoids and their pharmacological activity has led to a big growth of the market for cannabis-based products. This growth is mainly due to the commercialization of products based on cannabidiol (CBD). It is essential to differentiate between the terms hemp and marijuana to understand their molecular mechanisms. Although hemp refers to the species *Cannabis sativa* L. (Cannabaceae), the latter normally mentions to cultivars of cannabis with psychoactive (Δ9-tetrahydrocannabinol) potential used for both recreational and medicinal purposes [1]. Although *Cannabis sativa* L. is known by its phytocannabinoid composition, the phytochemical characterization reveals that are many other bioactive compounds such as phenolic compounds, alkaloids or lignanamides [2,3]. Particularly, phenolic compounds have been widely studied for their antioxidant

* Correspondence to: Facultad de Ciencias de la Salud, Universidad San Jorge, Campus Universitario Villanueva de Gállego Autovía A-23 Zaragoza-Huesca Km. 299. 50.830, Villanueva de Gállego, Zaragoza, Spain.
E-mail addresses: gcasedas@usj.es (G. Cásedas), ilopez@usj.es (V. López).

https://doi.org/10.1016/j.biopha.2026.119048
Received 17 October 2025; Received in revised form 13 January 2026; Accepted 21 January 2026
Available online 4 February 2026

properties; however, their role in hemp remains relatively underexplored. These metabolites, also known as polyphenols, contribute to the prevention of chronic disorders, as oxidative stress — a state categorized by an overproduction of reactive oxygen species (ROS) — damages proteins, lipids, and DNA; these alterations ultimately trigger apoptosis through mitochondrial dysfunction and caspase activation and is a key factor in the development of cardiovascular and neurodegenerative diseases [4,5]. Thus, antioxidants help reduce the risk of diseases through their ability to directly neutralize free radicals, chelate metal ions, and exert reducing power [6].

At cellular level, these metabolites increase the endogenous enzyme systems, which have antioxidant activities such as catalase (CAT), superoxide dismutase (SOD), glutathione peroxidase (GPx), glutathione reductase (GR) and peroxiredoxins (Prdx) [7–9]. In fact, anthocyanins like kuromanin and cyanidin-3-*O*-glucoside protect cultured cerebellar granule neurons from mitochondrial oxidative stress-induced apoptosis by preserving mitochondrial GSH and as a result, preventing cardiolipin oxidation and mitochondrial disintegration [10]. The expression of these antioxidant enzymes is regulated by nuclear factor erythroid 2-related factor 2 (Nrf2). NFE2L2 (Nrf2) regulates both oxidative stress and apoptosis, whose interplay is complex and context dependent. Even though, significant decreased nuclear Nrf2 levels have been detected in brain regions of patients with Alzheimer's disease [11]. Oxidative stress induces apoptosis through ROS-mediated damage and mitochondrial dysfunction, but activation of Nrf2 initiates a robust antioxidant response that mitigates this damage and suppresses apoptosis [12]. This dual role of Nrf2 as both a protector against oxidative damage in normal cells and a contributor to apoptosis resistance in cancer underscores its importance as a therapeutic target in diverse pathological conditions [13,14].

Several studies have demonstrated that polyphenols exert their neuroprotective effects by both directly scavenging free radicals and modulating intracellular signalling pathways. For instance, flavonoids such as quercitrin, phloretin and baicalein have been shown to mitigate ROS toxicity by reducing oxidative damage, normalizing mitochondrial function, and decreasing the activation of caspases associated with apoptosis [15]. Apoptosis in SH-SY5Y neuroblastoma cells is orchestrated by a complex interplay between stress-induced signalling pathways and mitochondrial regulatory proteins. The tumour suppressor protein *TP53* (p53) serves as a central mediator in this process by sensing cellular damage and initiating the transcription of pro-apoptotic factors, among which Bax is prominent, whereas the anti-apoptotic protein Bcl-2 acts to counterbalance this effect. Consequently, a shift in the Bax/Bcl-2 ratio toward Bax facilitates mitochondrial outer membrane permeabilization, cytochrome c release, and activation of caspase cascades that culminate in apoptotic cell death [16,17].

These compounds have been shown not only to restore the previous processes but also to reduce neuroinflammatory responses by modulating key signalling pathways that control cytokine production in neurodegenerative diseases [18,19]. At the molecular level, flavonoids modulate several intracellular signalling pathways implicated in oxidative stress and inflammation. Hesperetin, for example, activates the Nrf2/ARE antioxidant pathway while concurrently suppressing the TLR4/NF-κB and MAPK cascades, pathways that are central to the expression of pro-inflammatory cytokines such as IL-6 [20–22]. Activation of the sigma-1 receptor modulates neuroinflammation through multiple pathways. It attenuates proinflammatory signalling by restraining the overactivation of pathways such as the IRE1/XBP-1 cascade, leading to reduced secretion of cytokines including IL-6 and IL-8 [23,24].

Additionally, excessive nitric oxide (NO) production is a critical outcome of oxidative stress in SH-SY5Y neuronal cells that contributes to neuroinflammation, and cellular damage and flavonoids has also been shown to directly scavenge NO radicals in a dose-dependent manner. They directly scavenge reactive nitrogen species (RNS) and inhibit inflammatory signalling pathways by downregulating iNOS expression. This multi-layered mode of action not only reduces the biochemical markers of oxidative damage but also helps preserve neuronal integrity and function in the face of toxic insults [25,26]. Moreover, the broader literature supports the notion that by modulating redox-sensitive pathways and decreasing pro-inflammatory mediators, flavonoids contribute to a reduction in NO-mediated neurotoxicity. Such mechanisms underscore the therapeutic potential of flavonoids in counteracting neuroinflammation and oxidative stress associated with various neurodegenerative conditions [27–31].

The selection of cannabis as a polyphenol source in this study was primarily driven by the distinctive flavonoid profile of the extract, which is particularly enriched in flavones such as apigenin-7-*O*-glucuronide and luteolin-7-*O*-glucuronide. To the best of current knowledge, luteolin-7-O-glucuronide has not been previously investigated from cannabis in any neuroprotective assay, highlighting a relevant gap and a unique opportunity to explore its potential contribution to redox homeostasis and neuronal resilience. Furthermore, preliminary data from our laboratory demonstrate robust protection of neuronal cells against peroxide-induced mitochondrial dysfunction following treatment with this cannabis extract, providing additional support for prioritizing this matrix for in-depth mechanistic evaluation in the context of redox modulation and neuroprotection.

Hemp products and ingredients are usually used for its effects in the central nervous system due to psychoactive cannabinoids but in this study, the role of the phenolic fraction from *Cannabis sativa* L. is investigated in SH-SY5Y neuroblastoma cells using a combination of *in vitro* and *in silico* approaches for a better understanding of the subjacent cytoprotective effects and molecular mechanisms.

2. Materials and methods

2.1. Reagents and chemicals

The SH-SY5Y cell line was donated by the FunImmune group from the Basque Country University (UPV/EHU). High glucose Dulbecco's Modified Eagle's Medium (DMEM), Penicillin-Streptomycin, Phosphate Buffered Saline (PBS), Foetal Bovine Serum (FBS), Trypsin, 3-(4,5-dimethylthiazol-2-yl)-2 Bromide were acquired from Gibco. Sigma-Aldrich was the supplier of 5-Diphenyltetrazol (MTT), bicinchoninic acid (BCA), dimethyl sulfoxide (DMSO), Glucose, hydrogen peroxide (30 % w/w), RIPA lysis buffer. Bio-rad supplied Laemmli buffer, HRP-peroxidase and HSP90 antibodies while Nrf2, PRDX1, PRDX3, Sigma-1R antibodies and IL-6 kit (KE00139) were purchased from ProteinTech and IL-8 kit (A323171) from Antibodies (UK). Catalase (EIA-CATC) and superoxide dismutase (EIASODC) kits were bought from ThermoFisher.

2.2. Cannabis sativa material

Futura 75 hemp's frozen inflorescences, grown in Fiuminata, Central Italy, were utilized for extract production through microwave-assisted extraction (MAE) in water with a Milestone ETHOS X system (Milestone, Italy), as previously described and characterized by UHPLC-HRMS [3]. Finally, the phenolic fraction obtained from an aqueous extract (AE) from *Cannabis sativa* plant was developed for the following assays. This fraction is enriched in non-cannabinoid polyphenols, with apigenin, luteolin, kaempferol and quercetin derivatives, cannflavins A–C, and related flavonoid glycosides identified as the main constituents. Importantly, the fraction used in the cell-based assays is cannabinoid-depleted and specifically enriched in these non-cannabinoid polyphenols, which constitute the primary focus of the present study.

2.3. SH-SY5Y cell line

2.3.1. Cell culture

SH-SY5Y human neuroblastoma cells were thawed from a liquid nitrogen tank (using a 37ºC bath for 2–3 min) and cultured in high glucose DMEM supplemented with 10 % FBS and penicillin-streptomycin (2 mg/mL). They were then seeded in T25 flasks and placed in an incubator (maintained at 5 % CO2 and 37ºC) until reaching confluence. The cell culture medium was refreshed every three days. After passage, cells were seeded into 96-well plates at a density of 40,000 cells per well. Finally, cells were incubated for 24/48 h until reaching complete confluency in the well, allowing for subsequent treatment of the plate.

2.3.2. Cell treatments

Cells were pre-treated with lyophilized aqueous extract at concentrations ranging from 25 μg/mL to 1000 μg/mL for 24 h. Furthermore, a hydrogen peroxide stimulation (100 μM) was administered for 30 min to assess neuroprotective potential and promote an oxidative stress model. The study focused on evaluating protective effects at four concentrations (25–50–100–200 μg/mL), as these levels were found to be non-toxic in a previous publication.

2.3.3. Assessment of mitochondrial activity using the MTT assay

Following treatments, cell viability was assessed by incubating with MTT solution (2 mg/mL) for 2 h at 37°C. Subsequently, DMEM was removed, and DMSO was added to each well to dissolve formazan crystals. Absorbance was then measured at 550 nm using a Synergy H1 Multi-Mode Reader (Biotek) [32]. Each experiment was conducted five times, and the results were expressed as a percentage of the control (100 %).

2.3.4. Antioxidant defence (CAT, SOD, ROS)

Prior to assessing the activity of antioxidant enzymes, the protein content of SH-SY5Y cells was determined using a colorimetric bicinchoninic acid (BCA) assay, and then the lysate was normalized using a RIPA lysis buffer for 30 min. After that, the activity of catalase and superoxide dismutase was measured following the protocol described by the supplier. The activity was expressed in international units as mU/mL.

Neuroblastoma cells were simultaneously exposed to varying concentrations of hemp AE in the presence of hydrogen peroxide (100 μM). Intracellular reactive oxygen species (ROS) were quantified using DCFH-DA as a fluorescent probe, following the method originally described by LeBel et al. [33], with minor adaptations to our experimental conditions. ROS-dependent fluorescence was recorded at 37°C for 90 min, using an excitation wavelength of 480 nm and an emission wavelength of 510 nm using a Synergy H1 Multi-Mode Reader.

2.3.5. Protein expression by Western Blot

To assess the impact of polyphenolic hemp extract on the expression of Nrf-2, PRDX1, PRDX3 and Sigma-1R, SH-SY5Y cells were cultivated in Petri plates and treated with neuroprotective concentrations of the extract for 24 h. Subsequently, the cells were rinsed with PBS and lysed in a buffer or stimulated with hydrogen peroxide (100 μM) for 30 min. Lysates were then collected for protein quantification. Next, 30 μg of protein extract per sample was combined with Laemmli buffer containing beta-mercaptoethanol, loaded onto 10 % sodium dodecyl sulphate-polyacrylamide gel electrophoresis (SDS-PAGE), and transferred to nitrocellulose membranes. The membranes were promptly blocked with fat-free milk before being tested with the following antibodies: anti-Nrf-2 (80593–1-RR; ProteinTech, Manchester, UK), anti-Peroxiredoxin 1 (15816–1-AP; ProteinTech, Manchester, UK), anti-Peroxiredoxin 3 (66810–1-Ig; ProteinTech, Manchester, UK) and anti-Sigma-1R (15168–1-AP; ProteinTech, Manchester, UK). Antibody binding was detected by chemiluminescence with specific secondary antibodies labelled with horseradish peroxidase (HRP) (1706515, Bio-Rad, California, USA) and visualized on a C-DiGit Blot Scanner (LI-COR, Nebraska, USA) and Bio-Rad Molecular Imager ChemiDoc XRS (Bio-Rad, California, USA). Subsequently, blots were quantified using ImageJ software.

2.3.6. Quantitative real-time PCR

After the cell treatment in six-well plates, total RNA was extracted with an RNA extraction kit (740955.50, Macherey-Nagel, Dueren, Germany) according to the manufacturer's instructions. Then, expression values were determined by RT-qPCR using iTaq Universal SYBR Green Supermix (1725120, Bio-Rad, California, USA). To standardize the results, *RPLP0* was selected as the internal reference gene, and the expression levels of the target genes were calculated using the $2^{-\Delta\Delta CT}$ method. The primers used are shown in Table 1.

2.3.7. Determination of neuroinflammatory biomarkers

The NO content was measured by the Griess method, and the nitrite concentration in the medium was measured as an index of NO production. Cells were cultured in DMEM mixed with the indicated concentrations of aqueous extract, then exposed to H_2O_2 (100 μM) for 30 min. After 24 h, 100 μL of each supernatant was mixed with the same volume of Griess reagent (0.1 % N-1-naphthylethylenediamine hydrochloride in water and 1 % of p-aminobenzenesulfonamide in 5 % phosphoric acid, mix them in equal amounts). The reaction was protected from light at 37ºC for 15 min and the absorbance was measured at a wavelength of 540 nm [34]. $NaNO_2$ was selected as standard. The nitrite concentration was calculated with the $NaNO_2$ standard curve and expressed in μM.

IL-6 and IL-8 released in the cell supernatants were determined using ELISA kits according to the manufacturer's instructions. The concentration was calculated from the standard curve.

2.4. In silico methods

2.4.1. Molecular docking

Molecular docking was performed using the Nrf2 protein as receptor and the phenolic compounds identified in the aqueous fraction of *C. sativa* as ligands, running an independent docking analysis for each ligand-receptor pair.

For Nrf2 preparation, its three-dimensional structure was downloaded from AlphaFold [35]. Subsequently, it was examined in PyMOL and the active site was identified using Ghecom software, determining the center of mass at coordinates x: −27.532, y: 9.040, z: 35.144. The preparation protocol was completed in AutoDockTools [36], removing water molecules, adding polar hydrogens and applying Kollman charges [37]. As for the ligands, their structures were obtained from PubChem [38]. Each was visualized in PyMOL and subsequently prepared in AutoDockTools by a procedure that included water removal, ligand root definition, identification of rotatable bonds, addition of hydrogens and assignment of Gasteiger charges [39].

Molecular docking was carried out with the software AutoDock Vina, using a rigid receptor model to optimize computational performance. The size of the search box was set as twice the size of the ligand, with dimensions of x: 30, y: 30, z: 30. All calculations were executed was using an Ubuntu environment.

Table 1
Selected primers for in vitro tests.

Genes	Forward Primer (5'-3')	Reverse Primer (3'-5')
KEAP1	AAAGGAGACGATTGAGGACAGC	CTGCATCCACCACAACAGTG
RPLP0	GCAGCATCTACAACCCTGAAG	CACTGGCAACATTGCGGAC
P53	CCTCAGCATCTTATCCGAGTGG	TGGATGGTGGTACAGTCAGAGC
BCL2	GCCCTGTGGATGACTGAGTA	TTCAGAGACAGCCAGGAGAAA
BAX	CCCGACAGGTCTTTTTCCGAG	CCAGCCCATGATGGTTCTGAT
NFkB2	AGAGGCTTCCGATTTCGATATGG	GGATAGGTCTTTCGGCCCTTC

In addition, a complementary molecular docking analysis was performed using the Sigma-1 receptor (Sigma1R) and apigenin-O-glucuronide as a representative phenolic compound of the aqueous fraction of *C. sativa*. This exploratory analysis was conducted to preliminarily assess the potential involvement of alternative antioxidant pathways beyond Nrf2. Given the exploratory nature of this analysis, only a single, biologically relevant ligand was evaluated for Sigma1R. The Sigma1R structure was retrieved from the Protein Data Bank (PDB ID: 5HK1) [40], and the active site was defined based on previously reported literature [41]. All subsequent preparation steps were performed following the same protocol described above.

2.4.2. Molecular dynamics

Two molecular dynamics (MD) simulations were carried out using Gromacs to further investigate the stability and dynamic behavior of selected protein–ligand complexes. The first simulation involved the Nrf2 receptor in complex with apigenin-7-*O*-glucuronide, aiming to refine and characterize in greater detail the interaction previously identified by molecular docking within the main antioxidant pathway addressed in this study. The second simulation was performed on Sigma1R in complex with apigenin-7-*O*-glucuronide, with the purpose of exploratorily assessing the stability of the interaction in a potential alternative antioxidant-related pathway. In both cases, similar simulation protocols were applied. The systems were placed in a simulation box, followed by energy minimization, thermal (NVT) and pressure (NPT) equilibration, and production MD runs. Simulations were conducted at 300 K and 1 bar using the Verlet integrator with a time step of 2 fs for a total simulation time of 5 ns. Temperature coupling was performed using the V-rescale thermostat, and pressure coupling was applied using the isotropic Parrinello–Rahman barostat. Long-range electrostatic interactions were treated using the particle mesh Ewald (PME) method with a cutoff radius of 1.2 nm [42].

Trajectory analyses were performed to assess the structural stability and dynamic behavior of the system. These analyses included the calculation of the root mean square deviation (RMSD), root mean square fluctuation (RMSF) per residue, the radius of gyration (Rg), number of contacts, and the number of hydrogen bonds throughout the simulation. In addition, detailed visualization and inspection of the trajectories were conducted to monitor conformational changes and oligomeric rearrangements over time [43].

2.5. Statistical analysis

The results were analyzed using GraphPad Prism v.10 statistical software. Data were expressed as mean ± SEM from at least three independent experiments. The statistical significance of the results between each treated group was analyzed by one-way ANOVA, and the post-test was Dunnett's multiple comparisons test. Student *t*-test was also employed to evaluate differences between two groups. The difference was considered to be significant at $p < 0.05$.

3. Results

3.1. Effect of cannabis phenolic fraction on SH-SY5Y cell viability

Fig. 1A shows the non-toxicity effect of the cannabis phenolic fraction on SH-SY5Y cells at every concentration tested (25–200 μg/mL). After 24 h antioxidant treatment, neurons were exposed to hydrogen peroxide (100 μM) for 30 min, and cell viability was measured following a 23.5 h period. Fig. 1B displays significant differences at 25 and 50 μg/mL against hydrogen peroxide insult while 100 and 200 μg/mL improved mitochondrial activity compared to positive control.

3.2. Role of antioxidant key enzymes under redox conditions

The activity of catalase and superoxide dismutase (SOD) was quantified under oxidative stress conditions (Fig. 2). Positive control decreased catalase activity by more than half compared to control cells. But when cells were pretreated with cannabis phenolic fraction, the oxidative stress situation was counteracted and catalase activity was improved reaching significant differences at lower concentrations against hydrogen peroxide treatment (Fig. 2A).

On the other hand, cells treated solely with hydrogen peroxide exhibited an increase in superoxide dismutase activity (Fig. 2B), attributable to oxidative stress conditions. However, pretreatment with antioxidants did not significantly alter enzyme activity, although significant differences (100 and 200 μg/mL) were observed compared to the positive control.

3.3. The antioxidant response is ameliorated by the cannabis phenolic fraction

Western blotting was performed to determine the changes in the levels of Nrf2, PRDX1, and PRDX3 proteins. As shown in Fig. 3, the

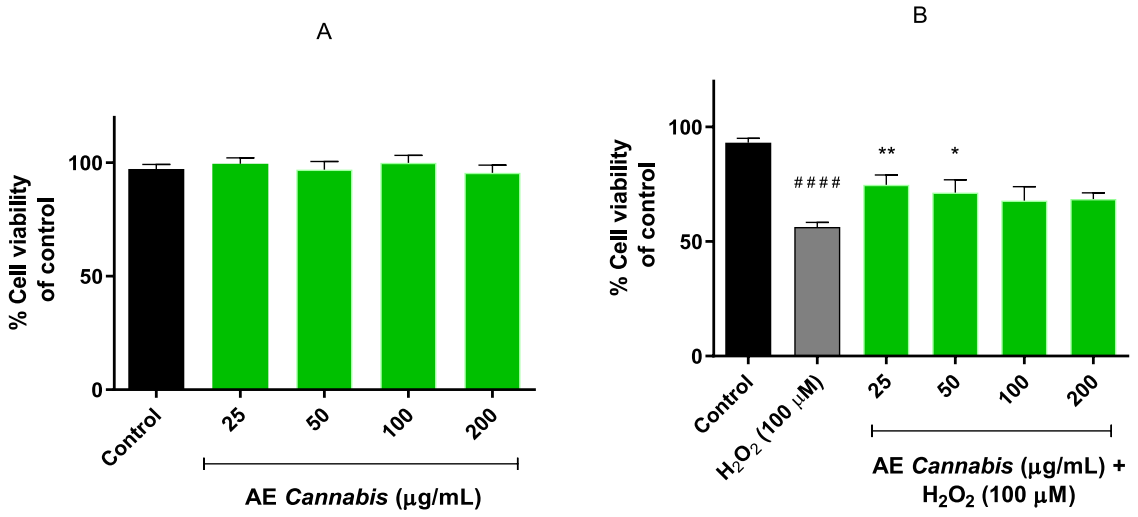

Fig. 1. Mitochondrial activity by the MTT assay. (A) Cell viability of SH-SY5Y neurons after exposure to different concentrations of cannabis phenolic fraction (AE *Cannabis*). (B) Cell viability modulation by cannabis phenolic fraction (AE *Cannabis*) in response to hydrogen peroxide (100 μM)-induced oxidative stress. Note: #### $p < 0.0001$ *versus* control. Significant differences appeared at 25 μg/mL ($p < 0.05$) and 50 μg/mL ($p < 0.01$) over positive control cells.

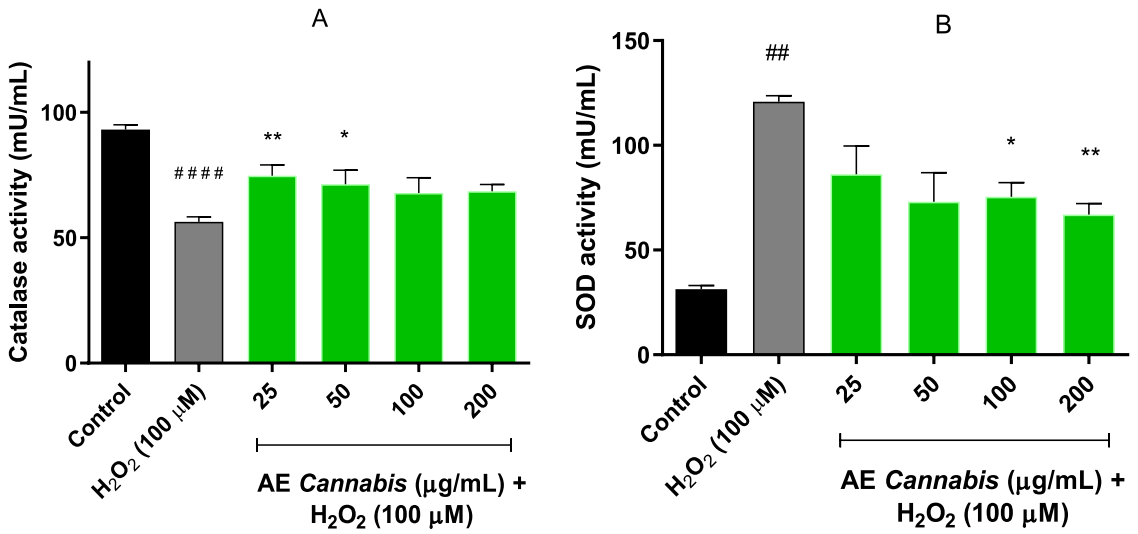

Fig. 2. Catalase and superoxide dismutase activity in response to cannabis phenolic fraction (AE Cannabis) and H_2O_2-induced oxidative stress. (A) Catalase activity in SH-SY5Y cells (B) SOD activity in SH-SY5Y cells. Note: ## $p < 0.01$ and #### $p < 0.0001$ *versus* control; * $p < 0.05$ and ** $p < 0.01$ *versus* hydrogen peroxide.

antioxidant response on SH-SY5Y neurons was successfully demonstrated as Nrf2, PRDX1 and PRDX3 levels were highly increased over control cells subjected to the cannabis phenolic fraction. Complementary, the expression of *KEAP1* mRNA was not altered at the concentrations tested (Fig. 3B). A trend in the decrease of *KEAP1* levels (Fig. 4D) could result in the stabilization and activation of Nrf2 at selected concentrations, leading to increased expression of antioxidant enzymes and proteins that help protect cells from oxidative stress and maintain redox homeostasis. Moreover, the expression of the master regulator of antioxidative response – Nrf2 – not only enhanced when cells were stimulated with hydrogen peroxide but also exerted significant differences in comparison to both positive and negative (Fig. 3F). ROS quantification corroborated the antioxidant capacity of AE cannabis (Fig. 3H). In this 90-min assay, SH-SY5Y cells were co-exposed to increasing concentrations of AE and hydrogen peroxide from T = 0, thereby directly challenging the extract under sustained pro-oxidant conditions. AE consistently maintained ROS levels below those of the positive control from 40 min onwards and up to the end of the experiment, particularly at concentrations between 25 and 100 μg/mL. Notably, ROS values exhibited a progressive decline at later time points, approaching those observed in untreated control cells.

3.4. Apoptotic regulation by cannabis phenolic fraction through the p53–Bcl-2/Bax signalling pathway in SH-SY5Y cells

Fig. 4 reveals the mRNA expression of apoptotic biomarkers p53, Bcl-2 and Bax by RT-qPCR. The redox-regulated transcription factor, p53, boasts a multitude of cellular roles, garnering increasing interest within the realm of neurodegenerative diseases. At lower levels of oxidative stress, p53 encourages antioxidant actions, leading to enhanced cell survival. Fig. 4A illustrates how this cannabis extract modulates the antioxidant response mediated by p53. While Bcl-2 regulates apoptosis, there is some evidence suggesting that it may also be involved in modulating oxidative stress responses. In this case, the phenolic fraction obtained from *Cannabis sativa* moderately rose up Bcl-2 levels confirming antiapoptotic effect as previously regulated mitochondrial activity (Fig. 4B). By decreasing Bax levels (Fig. 4C), most of the concentrations could reduce apoptosis, leading to enhanced cell survival and protection against cell death as other protein results revealed. In aggregate, Fig. 4D shows the antiapoptotic effect of Cannabis phenolic fraction on the Bax/Bcl2 ratio.

3.5. Phenolic compounds from Cannabis sativa as modulators of neuroinflammation

Fig. 5 represents the neuroinflammation model on SH-SY5Y cells via NO production, cytokine determination, Sig-1R protein quantification and NFκB2 mRNA expression. Through Griess reaction, NO production was reduced in cell supernatants treated both cannabis phenolic fraction and H_2O_2 when compared to supernatant exposed only to hydrogen peroxide (Fig. 5A). Significant differences were reached at every concentration tested. On the other hand, IL-6 levels increased, while IL-8 levels decreased as a part of oxidative stress response (Fig. 5B, C). This increase in IL-6 could represent a feedback mechanism aimed at restoring cellular homeostasis and promoting tissue repair according to results on NF-κB2 expression (Fig. 5D). The NF-κB2 effect increases in a dose-dependent manner to the polyphenolic extract, indicating a potential anti-inflammatory and antioxidant feature. Finally, western blotting revealed that under basal conditions, Sigma-1R expression is significantly reduced compared to the control, whereas under oxidative stress, the expression of this protein decreases in a dose-dependent manner (Fig. 5E, F).

3.6. Computational analysis of phenolic compounds from Cannabis sativa and the binding mode between Nrf-2 and KEAP1 and Sigma-1R

3.6.1. Molecular docking

The molecular interactions between the most abundant compounds in the *C. sativa* aqueous fraction and the Nrf2 protein were analyzed through molecular docking studies. The aim was to predict binding affinity and characterize the specific interactions each ligand establishes with the residues of Nrf2's active site, distinguishing between hydrogen bonds and hydrophobic interactions.

The results revealed binding affinities ranging from moderate to high, with values between –8.068 kcal/mol and –4.364 kcal/mol. The compound with the highest affinity was apigenin C-(hexoside-*O*-rhamnoside), which exhibited a high number of hydrophobic interactions, although it formed relatively few hydrogen bonds. In contrast, compounds such as eriodictyol-7-*O*-glucoside, luteolin-7-*O*-glucuronide, apigenin glucuronide, and *O*-methyl luteolin glucuronide showed slightly lower—yet still notable—affinities and were characterized by a greater number of hydrogen bonds.

In general, the ligands with the highest affinities formed multiple interactions with key residues in the Nrf2 binding site, particularly Asp283, Leu583, Gln584, Tyr286, Thr279, and Gly282. Additionally,

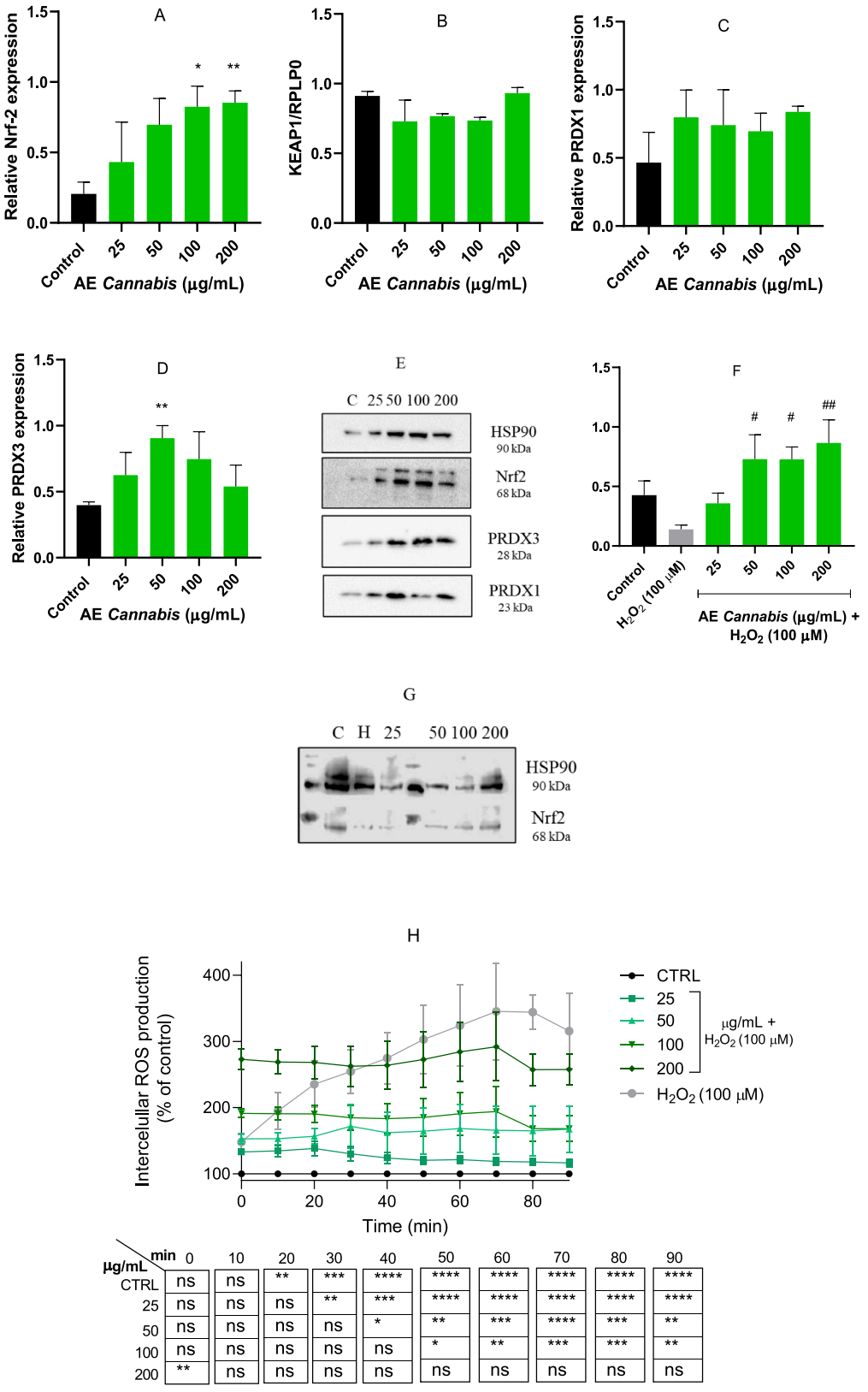

µg/mL \ min	0	10	20	30	40	50	60	70	80	90
CTRL	ns	ns	**	***	****	****	****	****	****	****
25	ns	ns	ns	**	***	****	****	****	****	****
50	ns	ns	ns	ns	*	**	***	****	***	**
100	ns	ns	ns	ns	ns	*	**	***	***	**
200	**	ns	ns	ns	ns	ns	ns	ns	ns	ns

Fig. 3. Cannabis phenolic fraction (AE Cannabis) modulates the antioxidant response in SH-SY5Y cells by induction of nuclear factor erythroid 2-related factor 2, peroxiredoxin 1 and 3. Nrf2 (A, F), PRDX1 (C) and PRDX3 (D) expressions were determined by Western blot and expressed as protein densitometry. (B) Expression of the *KEAP1* mRNA by RT-qPCR. (E) Total protein expression levels in SH-SY5Y cells. (G) Total Nrf2 expression levels in hydrogen peroxide-induced SH-SY5Y cells. (H) ROS production in SH-SY5Y cells insulted with hydrogen peroxide (100 µM) and treatments with *Cannabis sativa* aqueous extract (25–200 µg/mL). Data are expressed as percentage over control cells and the assay was carried out for 90 min in order to measure intracellular ROS production. Note: # $p < 0.05$ and ## $p < 0.01$ *versus* hydrogen peroxide; * $p < 0.05$ and ** $p < 0.01$ *versus* control.

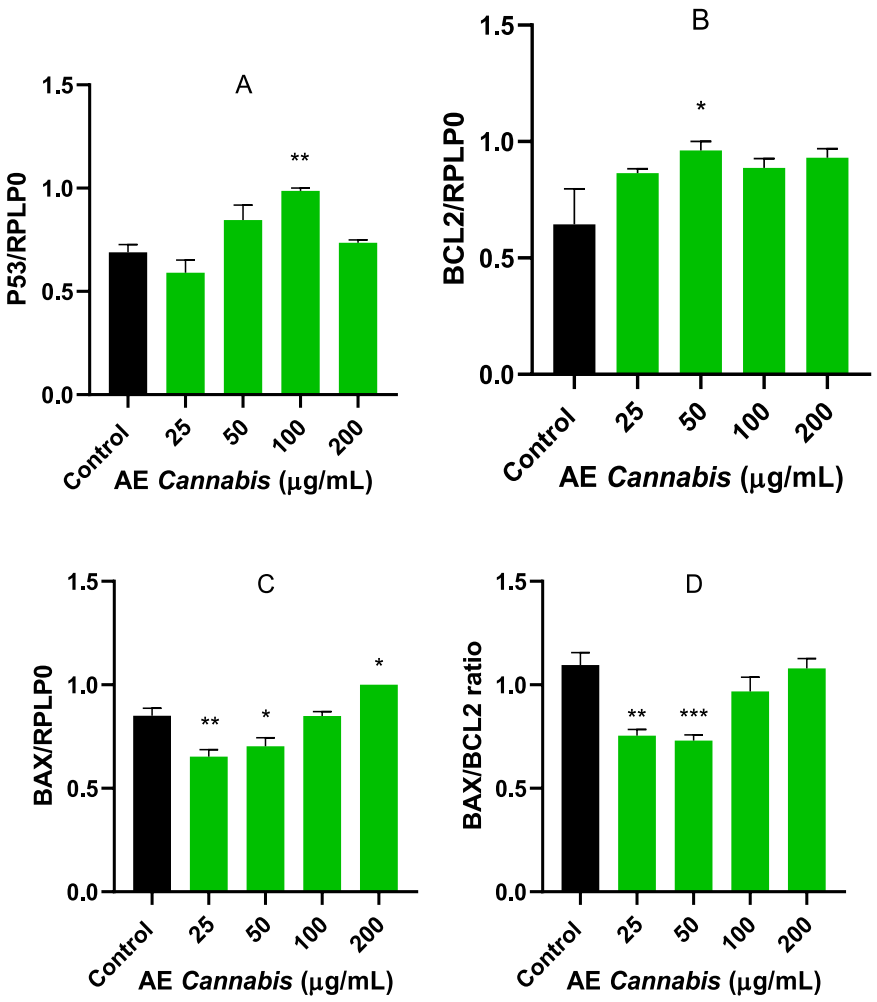

Fig. 4. Expression of apoptosis-related genes (A) *P53*, (B) *BCL2*, and (C) *BAX* relative to *RPLP0* (D) BAX/BCL2 ratio and the modulatory effect of polyphenolic cannabis extract antioxidants. Note: * $p < 0.05$, ** $p < 0.01$ and *** $p < 0.001$ *versus* control.

compounds like luteolin di-C-hexoside and vitexin-200-*O*-glucoside demonstrated a large number of hydrophobic interactions, complemented by several hydrogen bonds. Notably, the frequent involvement of residue Leu583 in hydrophobic interactions appears to play a fundamental role in stabilizing the docking between the ligands and the Nrf2 protein (Figs. 6 and 7).

To further explore the potential involvement of alternative antioxidant-related pathways, molecular docking was additionally performed between apigenin-7-*O*-glucuronide and Sigma1R. As shown in Table 2, apigenin-7-*O*-glucuronide exhibited a favourable predicted binding affinity toward Sigma1R (–10.09 kcal/mol), forming multiple stabilizing interactions within the putative binding region (Fig. 8). Specifically, the ligand established five hydrogen bonds involving residues Tyr103, Ser117, Tyr120, and Thr181, along with five hydrophobic contacts primarily with Phe107, Tyr120, Ile124, His154, and Ala185.

Despite the favourable docking score and the presence of multiple non-covalent interactions, structural inspection of the Sigma1R binding site revealed a pronounced steric hindrance that partially occludes the ligand binding cavity. This suggests that, under physiological conditions, ligand access to the predicted binding site may require conformational rearrangements of the receptor. Therefore, although the docking results indicate a thermodynamically favourable interaction, they may not fully reflect a biologically accessible binding event in a rigid receptor model. To address this limitation and to evaluate whether receptor flexibility could enable or stabilize ligand binding, molecular dynamics simulations were subsequently performed.

3.6.2. Molecular dynamics

Because of the high computational cost associated with the system, the molecular dynamics simulation was limited to a few nanoseconds, which did not allow for exhaustive conformational sampling. Nevertheless, these preliminary results provide a foundation for future extended simulations, with a planned duration of at least 50 ns.

a) Nrf2 and apigenin-7-*O*-glucuronide complex molecular dynamics

The RMSD of Nrf2 shows a rapid initial increase to 2 nm within the first 0.5 ns, followed by a progressive rise with moderate fluctuations, reaching values between 2.5 and 4.5 nm after 1 ns without clear stabilization by the end of the trajectory. RMSF analysis reveals heterogeneous residue mobility, with most residues displaying moderate fluctuations (3–6 Å) and pronounced flexibility peaks in specific regions, particularly residues 350–400 and the C-terminal region (residues 580–610), where RMSF values reach 12–14 Å. Contact analysis indicates that the ligand maintains intermittent interactions with the protein throughout most of the simulation, with transient reductions in the number of contacts observed around 2.5 ns; however, hydrogen bond analysis reveals a consistently low frequency of ligand–protein hydrogen bond formation. The radius of gyration exhibits higher values along the X and Z axes compared to the Y axis, indicating a more extended conformation in these directions while remaining relatively compact along Y, reflecting a redistribution of the protein conformation without abrupt structural changes. Analysis of the MD trajectory further shows the progressive approach of apigenin-7-*O*-glucuronide toward Nrf2; however, the limited simulation time does not allow the establishment

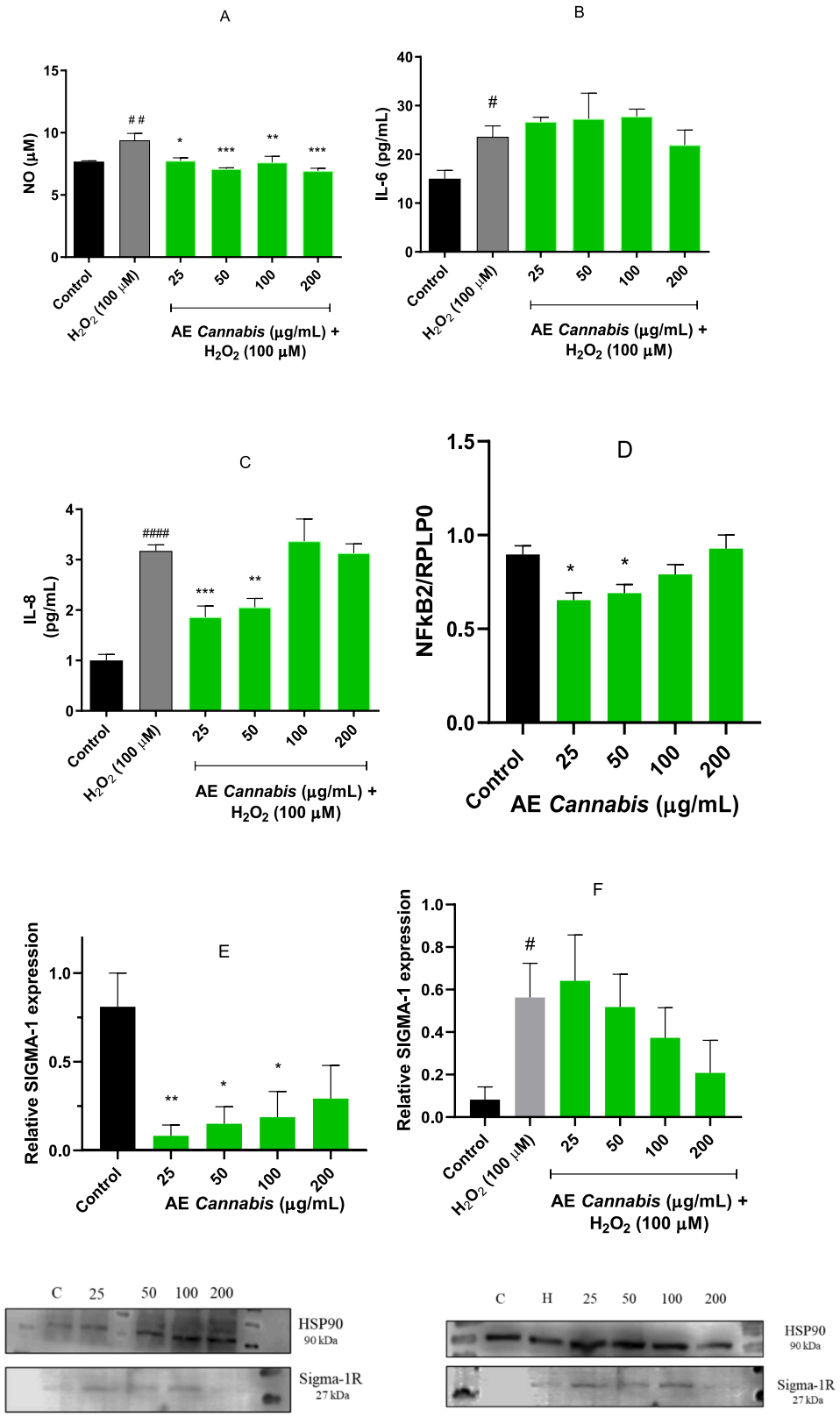

Fig. 5. Anti-inflammatory and redox-modulating effects of cannabis phenolic fraction. (A) Nitric oxide (NO) production was quantified in cell supernatants using the Griess assay to assess nitrosative stress levels. (B, C) Cytokines IL-6 and IL-8 were quantified by ELISA. (D) Relative expression of *NFKB2* mRNA, a central regulator of inflammation and redox signalling, was analyzed by RT-qPCR and normalized to *RPLP0*. (E, F) Sigma-1 receptor (Sigma-1R) protein levels were quantified under different treatment conditions by Western blot, as a potential marker of redox homeostasis and cellular stress response. Note: # $p < 0.05$; ## $p < 0.01$ and #### $p < 0.0001$ *versus* hydrogen peroxide; * $p < 0.05$; ** $p < 0.01$ and *** $p < 0.001$ *versus* control.

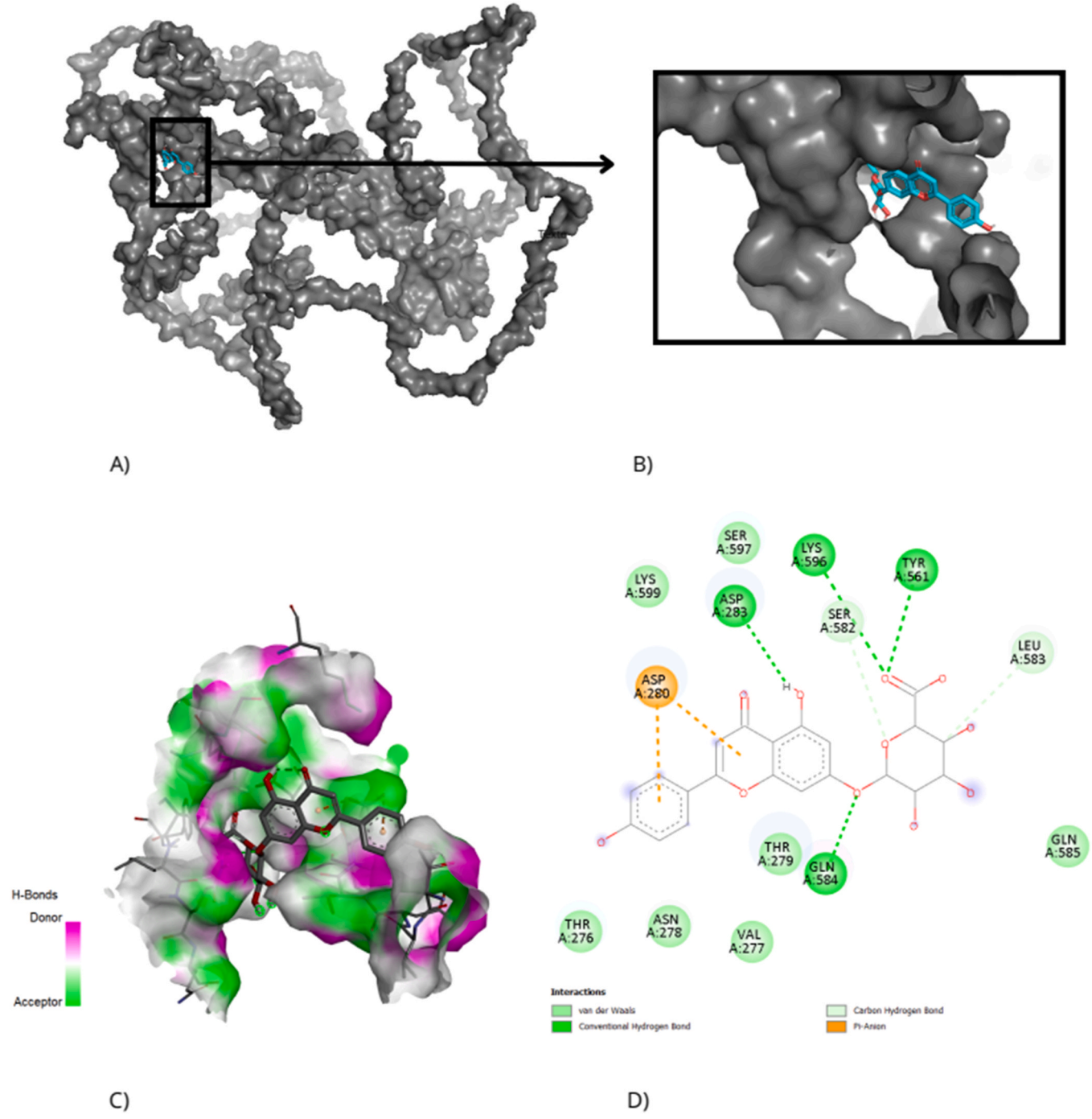

Fig. 6. Molecular docking model of apigenin-7-*O*-glucuronide with the Nrf2 protein. A) General three-dimensional representation of the interaction. B) Close-up of the three-dimensional model at the interaction site. C) Hydrogen-bond interactions within the active site. D) Two-dimensional interaction diagram.

of a stable interaction with the active site to be conclusively observed, highlighting the need for longer simulations (Fig. 9).

b) Sigma1R and apigenin-7-O-glucuronide complex molecular dynamics

RMSD increased rapidly at the initial stage, reaching values close to 10 nm and remaining stable for the rest of the trajectory, with a transient fluctuation observed around 0.6 ns, indicating overall structural stabilization. The RMSF profile revealed predominantly moderate residue mobility (4–7 Å), with localized regions of increased flexibility around residues 210–230 and a pronounced maximum in the 420–450 region, whereas residues 470–600 exhibited the lowest fluctuations, consistent with relatively rigid segments. Contact analysis revealed a sharp increase in the number of protein–ligand contacts within the first 0.3 ns, indicating an early intermolecular encounter, followed by a progressive loss of contacts that persisted throughout the remainder of the simulation, with only transient contact fluctuations observed thereafter. The number of hydrogen bonds remained low overall, predominantly between 0 and 2, with a transient increase to a maximum of three hydrogen bonds between 0.4 and 0.9 ns. The radius of gyration remained globally stable, with average values of approximately 2.4 nm along the X and Y axes and 2.5 nm along the Z axis; transient peaks were observed at the beginning of the trajectory and around 0.6 ns, after which values rapidly returned to baseline. The initial peak coincided with a conformational rearrangement of SigmaR1 associated with a

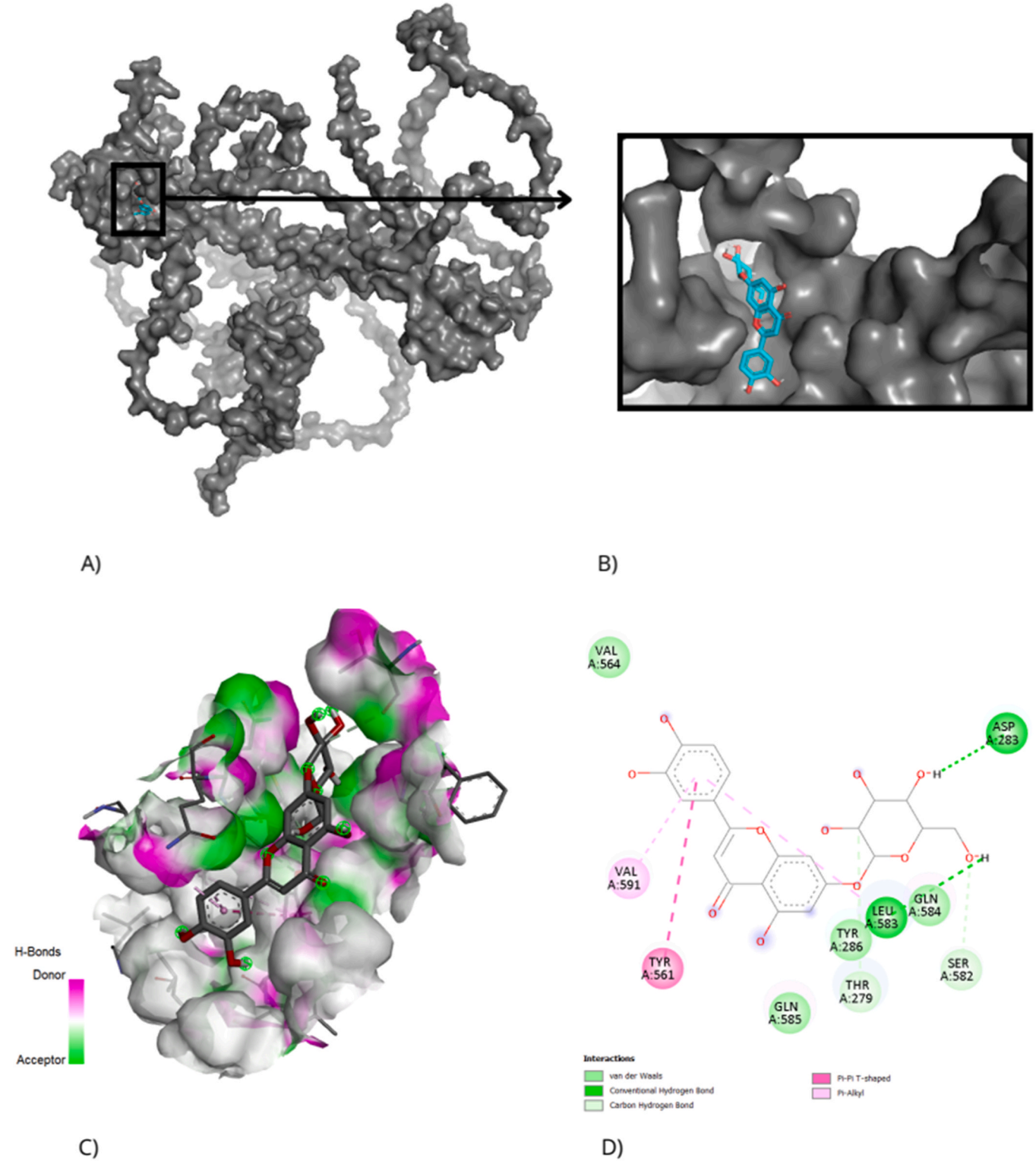

Fig. 7. Molecular docking model of luteolin-7-*O*-glucuronide with the Nrf2 protein. A) General three-dimensional representation of the interaction. B) Close-up of the three-dimensional model at the interaction site. C) Hydrogen-bond interactions within the active site. D) Two-dimensional interaction diagram.

transition from a dimeric to a trimeric state. No sustained changes in global protein compactness were detected, and the trajectory reflects a clear ligand-induced structural reorganization, progressing from an initially disordered and flexible state toward a more compact, trimeric assembly with ligand stabilization at the intersubunit interface (Fig. 10).

4. Discussion

Considering the central role of oxidative processes in the pathogenesis of various diseases, along with the potent *in vitro* antioxidant capacity exhibited by many phenolic compounds, it is reasonable to propose a link between the antioxidant properties of dietary polyphenols and the prevention of certain diseases [44]. In this study, it was

Table 2
Molecular docking results including binding affinity (kcal/mol), hydrogen bond interactions, and hydrophobic contacts between ligands and target protein residues.

Molecular Docking	Binding affinity (kcal/mol)	Number of Hydrogen bonds	Residues involved in Hydrogen bonding	Number of amino acids involved in hydrophobic interactions	Residues involved in hydrophobic interactions
Nrf-2					
Apigenin 6,8-di-C-glucoside	-6.824	1	Asp283	14	Phe281, Phe285, Tyr286, Asp283, Tyr561, Gly282, Ser582, Leu583 (2), Thr279 (2), Gln584, Gln585 (2)
Luteolin di-C-hexoside	-7.706	6	Leu583, Asp283 (2), Gln585 (2), Thr279	14	Tyr256, Tyr261, Phe281, (3), Phe285 (3), Gly282, Thr586, Gln584, Tyr286, Leu583, Gln585
Luteolin C-(hexoside-O-rhamnoside)	-7.667	6	Leu583 (2), Thr279, Val277 (2), Ser597	14	Ser582, Leu583, Gln584, Tyr286, Thr279, Val277 (2), Asn278, Thr276 (2), Asp280, Asp288 (2), Lys596
Vitexin-2"-*O*-glucoside	-7.425	4	Thr279, Leu583, Gln585 (2)	14	Lys554, Phe281 (2), Phe285 (2), Asp283, Thr279, Gly282, Leu583 (2), Tyr286, Leu537, Tyr551, Gln584, Gln585
Apigenin C-(hexoside-*O*-rhamnoside)	-8.068	2	Phe281, Tyr286	14	Phe281 (2), Phe285, Leu557, Gly582, Val591, Tyr286, Gln585 (2), Gln584, Asp283 (2), Ser582, Leu583
Eriodictyol-7-*O*-glucoside	-7.583	6	Leu583 (2), Try561, Ser582, Asp283, Thr279	13	Val564, Leu560, Leu557, Val591 (2), Tyr286, Leu583 (2), Tyr561, Ser582, Asp283, Thr279, Gln584
Luteolin-7-*O*-glucuronide	-7.387	6	Ser582, Asp283, Thr279, Tyr561, Leu583 (2)	12	Asp283, Ser582, Leu583 (2), Tyr561, Gln584, Thr279, Tyr286, Leu557, Leu560, Val591, Val564
Apigenin glucuronide	-7.397	5	Leu583 (2), Tyr561, Thr279, Gln584	11	Tyr561, Tyr286, Gly282, Leu583, Gln584, Ser582, Asp283, Asp280, Thr279, Val277, Thr276
O-Methyl luteolin glucuronide	-7.462	3	Gln585, Asn278, Thr279	10	Gln585, Leu583, Gly282, Gln584, Tyr286, Thr279, Asn278, Asp283, Asp280, Ser582
Caffeoyl-*O*-hexoside	-6.699	3	Thr279 (2), Asp283	12	Thr279, Asp283, Gly282, Ser582, Tyr561, Tyr286, Leu583 (2), Val564, Leu560, Leu557, Gln585
Protocatecuic acid hexoside	-6.189	6	Asp283 (2), Ser582 Thr279 (2), Leu583	12	Asp283, Ser582, Thr279, Gly282, Tyr286, Tyr561, Gln584 (4), Gln585, Leu583
Citric acid	-4.364	3	Tyr561, Leu583 (2)	8	Tyr561, Asp283, Ser582, Tyr286, Leu583, Gly282, Thr279, Gln584
Sigma 1 R					
Apigenin glucuronide	-10.09	5	Try103, Ser117, Tyr120 (2), Thr181,	5	Phe107, Tyr120, Ile124, His154, Ala185

demonstrated that phenolic compounds from *Cannabis sativa* can modulate antioxidant response not only under oxidative stress conditions but also in basal conditions, providing novel *in vitro* and *in silico* evidence for the role of *Cannabis sativa* phytochemicals in redox regulation and neuronal protection.

The phenolic fraction from *Cannabis sativa* comprises a diverse array of bioactive molecules, including flavonoids such as apigenin, luteolin, kaempferol, quercetin and rutin derivates as well as unique methylated flavones (cannflavins A, B, and C), that collectively exhibit potent antioxidant activities [3,45]. Flavonoids represent a diverse class of phenolic compounds that have been extensively shown to afford neuroprotection in SH-SY5Y neuroblastoma cells by mitigating oxidative stress, reducing apoptosis, and suppressing inflammation [46,47]. In these neuronal models, treatments with flavonoids such as quercetin, naringenin and afzelin have consistently decreased reactive oxygen species (ROS) production and lipid peroxidation while enhancing cell viability against oxidative challenges induced by agents like hydrogen peroxide (H_2O_2), cyclophosphamide, and 6-hydroxydopamine, according to the results obtained in this manuscript [47–49]. Thus, antioxidant polyphenols can act non-specifically by scavenging or modulating ROS, or specifically by inhibiting enzymes or enhancing antioxidant defences (catalase, SOD, peroxiredoxins). Their ROS-scavenging activity is mainly due to hydroxyl groups on the aromatic ring, which can donate a hydrogen atom or electron to stabilize reactive species [50,51]. Evidence from studies using SH-SY5Y cells indicates that flavonoids such as naringenin enhance the activities of both SOD and catalase, thereby contributing to the attenuation of oxidative stress and the stabilization of cellular homeostasis [46,52]. This could explain the results achieved in this study for catalase activity. In contrast to previous studies that suggested a decreased in SOD activity after hydrogen peroxide insult, our results indicate that a rise in the enzyme activity, suggesting an alternative or complementary mechanism involving Nrf2/ARE axis activation.

In addition to these traditional antioxidant enzymes, peroxiredoxins—specifically PRDX1 and PRDX3—play pivotal roles in reducing peroxides and maintaining redox balance in neuronal cells. PRDX1, primarily a cytosolic enzyme, has been associated with protecting SH-SY5Y cells against toxic insults; its inhibition leads to increased susceptibility to oxidative damage and apoptotic cell death. Mitochondrial PRDX3, on the other hand, is essential for detoxifying hydrogen peroxide within the mitochondria, and its diminished function is correlated with exacerbated oxidative injury under neurodegenerative conditions [53]. Although the direct modulation of PRDX1 and PRDX3 by flavonoids has not been explicitly detailed in the provided excerpts, the robust antioxidant capacity attributed to flavonoid treatments in SH-SY5Y cells implies possible preservation or upregulation of these peroxiredoxin systems [49]. In some studies, treatment with flavonoid-rich extracts not only reduced the markers of oxidative damage but also increased the activities of endogenous antioxidants, suggesting a synergistic interplay among catalase, SOD, PRDX1, and PRDX3 that fortifies neuronal cells against cytotoxic oxidative insults [49,52].

An increasingly recognized mechanism by which polyphenols exert antioxidant effects *in vivo* involves their ability to modulate the expression of the previous named antioxidant enzymes through activation of the Keap1/Nrf2/ARE pathway. In that way, molecular docking studies performed between the major compounds of *Cannabis sativa* extract and the Nrf2 protein revealed relevant interactions that may have functional implications in the modulation of the antioxidant Keap1/Nrf2 pathway. Overall, a moderate to high binding affinity was observed between the evaluated ligands and the active site of Nrf2, with

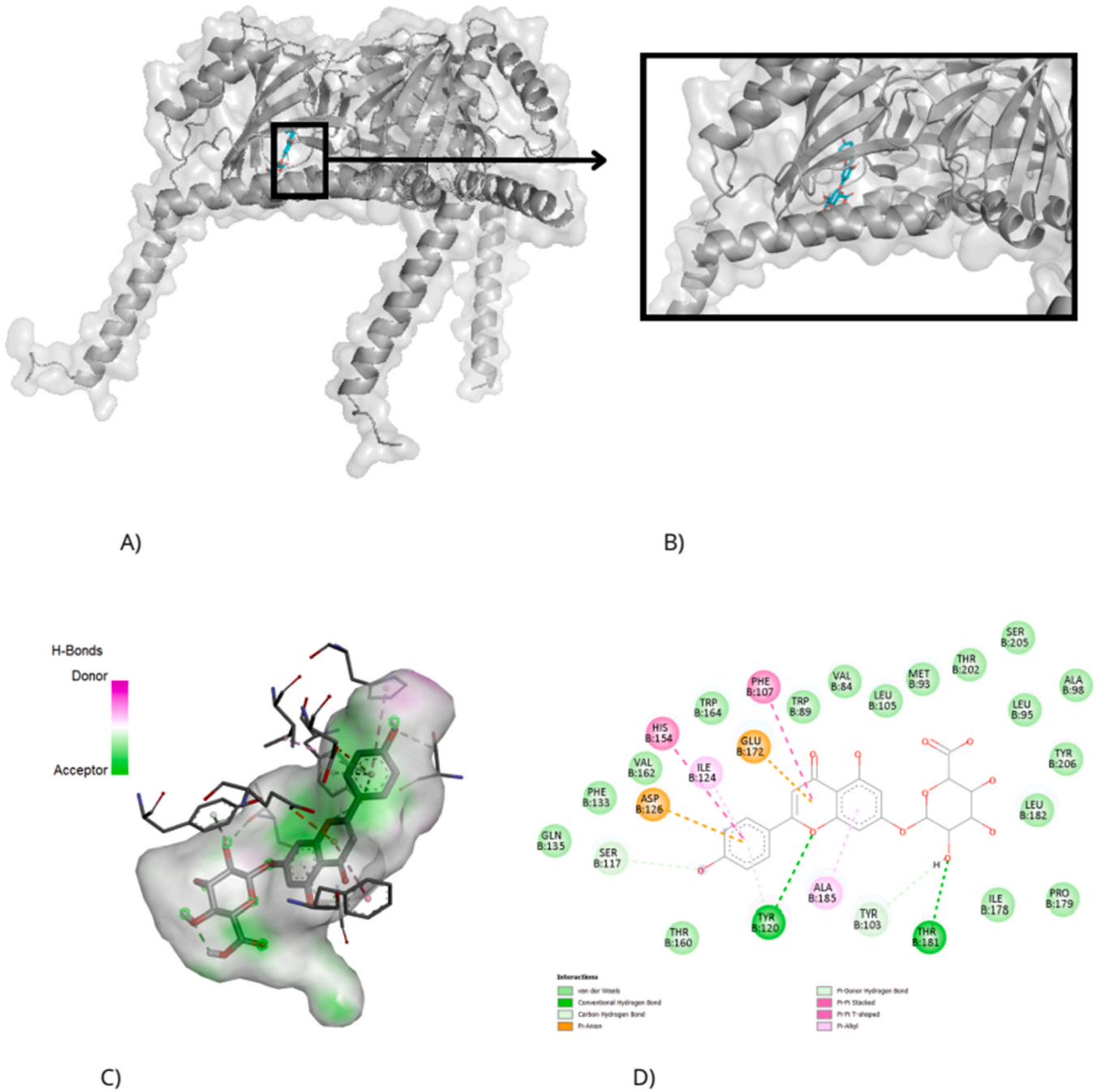

Fig. 8. Molecular docking model of apigenin-7-*O*-glucuronide with the Sigma1R protein. A) General three-dimensional representation of the interaction. B) Close-up of the three-dimensional model at the interaction site. C) Hydrogen-bond interactions within the active site. D) Two-dimensional interaction diagram.

binding free energy values ranging from −8.068 kcal/mol to −4.364 kcal/mol. These results suggest the potential of these secondary metabolites to interact stably with the protein.

The compound with the highest affinity was apigenin-C-hexoside-O-rhamnoside (-8.068 kcal/mol), whose interaction was characterized by a network of hydrophobic contacts with key residues of the binding site, particularly Phe281, Phe285, Tyr286, Gln584, and Leu583. Despite forming only two hydrogen bonds, the large number of nonpolar interactions appears to have significantly contributed to complex stabilization, consistent with the well-established importance of hydrophobic interactions in ligand–protein recognition at aromatic residue-rich sites [54]. Compounds such as luteolin di-C-hexoside, eriodictyol-7-*O*-glucoside, and luteolin-7-*O*-glucuronide exhibited slightly lower affinities but formed a greater number of hydrogen bonds. In particular, luteolin di-C-hexoside established six hydrogen bonds with residues including Leu583, Asp283, Gln585, and Thr279 [55–57]. Notably, Leu583 was recurrently involved in almost all high-affinity complexes, reinforcing its role as a key anchoring point within the Nrf2 binding site. Additionally, compounds such as vitexin-2”-*O*-glucoside, luteolin C-(hexoside-O-rhamnoside), and apigenin glucuronide showed a balance between hydrophobic contacts and hydrogen bonding, with similarly high affinities. These results suggest that the presence of glucuronide or rhamnoside substituents may facilitate the establishment of multiple contacts, thereby enhancing binding versatility.

Conversely, the compound with the lowest affinity, citric acid (-4.364 kcal/mol), formed fewer interactions with the receptor, which may be attributed to its structure providing lower steric complementarity with the Nrf2 active site.

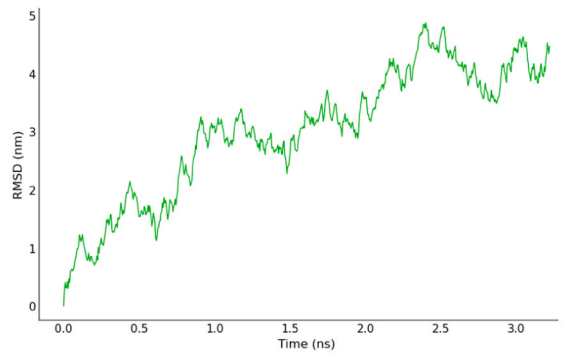

A)

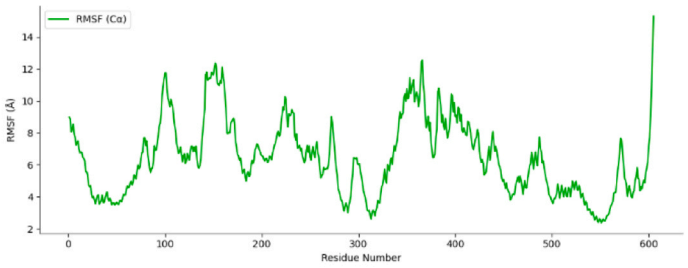

B)

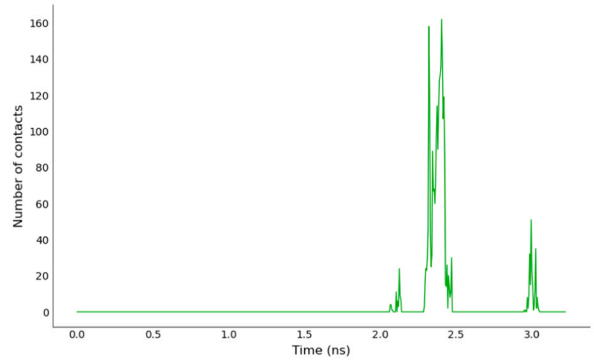

C)

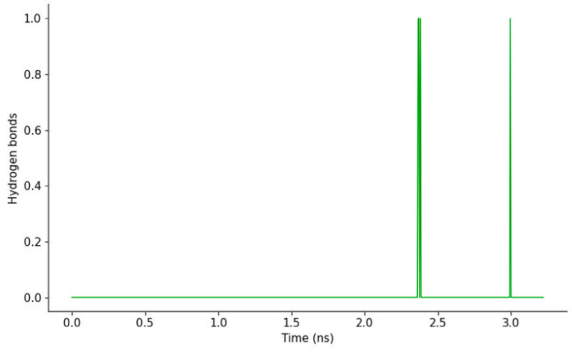

D)

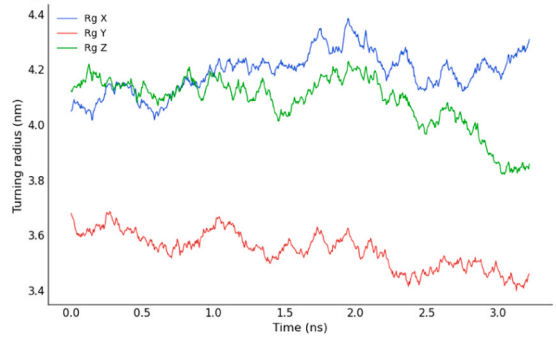

E)

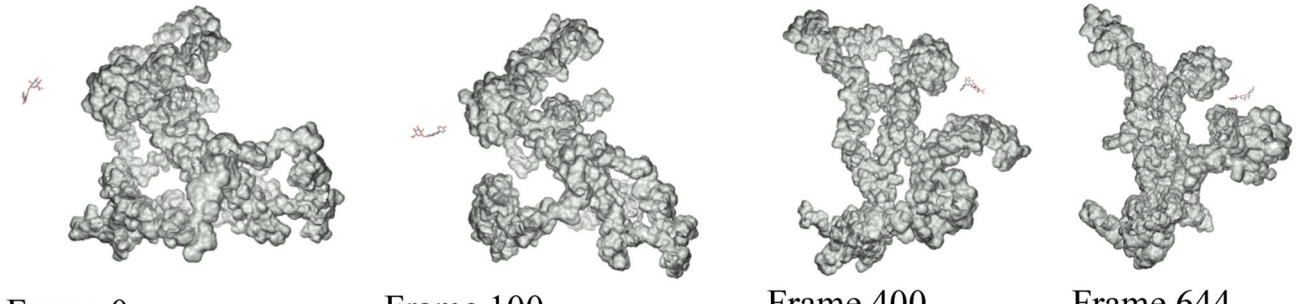

F)

Fig. 9. Molecular dynamics analysis of the Nrf2–Apigenin-7-*O*-glucuronide system. A) Root mean square deviation (RMSD). B) Root mean square fluctuation (RMSF) per residue. C) Minimum distance between the ligand and the receptor. D) Number of hydrogen bonds formed between Nrf2 and the ligand. E) Radius of gyration of Nrf2. F) Representative MD trajectory showing the relative movement of apigenin-7-*O*-glucuronide with respect to Nrf2.b) Sigma1R and apigenin-7-*O*-glucuronide complex molecular dynamics.

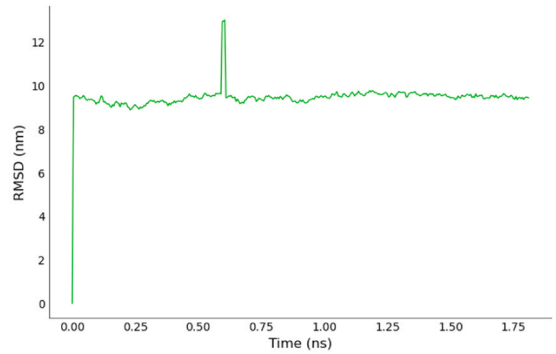

A)

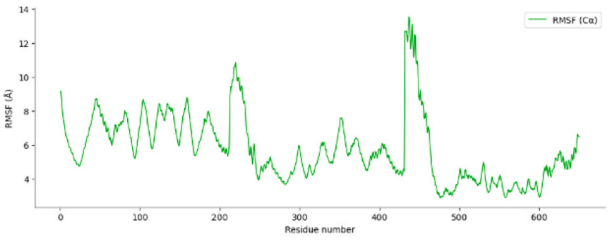

B)

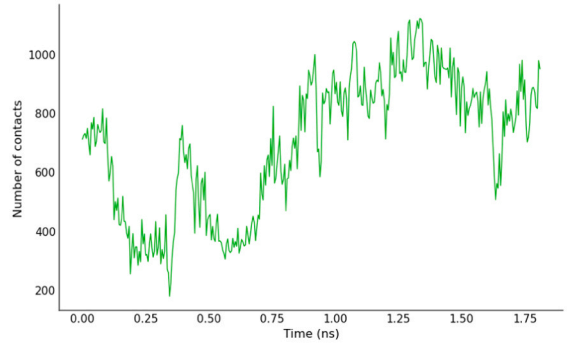

C)

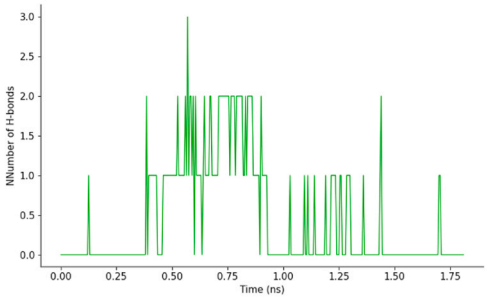

D)

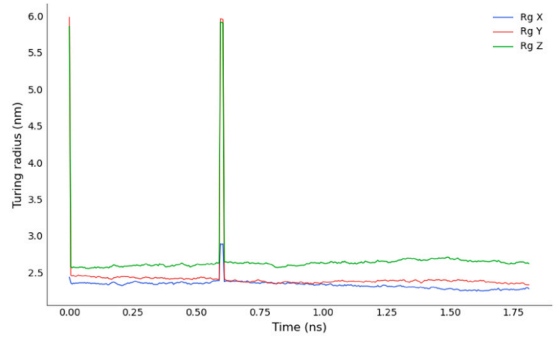

E)

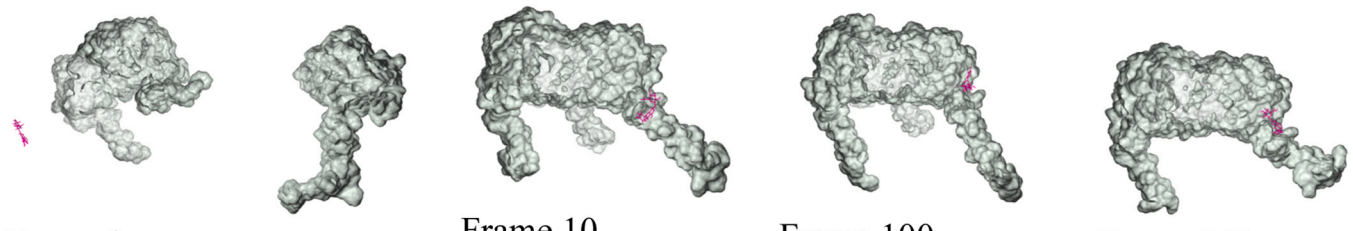

F)

Fig. 10. Molecular dynamics analysis of the Sigma1R–Apigenin-7-*O*-glucuronide system. A) Root mean square deviation (RMSD). B) Root mean square fluctuation (RMSF) per residue. C) Minimum distance between the ligand and the receptor. D) Number of hydrogen bonds formed between Sigma1R and the ligand. E) Radius of gyration of Sigma1R. F) Representative MD trajectory showing the relative movement of apigenin-7-O-glucuronide with respect to Sigma1R.

These findings indicate that various flavonoids present in *C. sativa* exhibit a strong capacity to interact with Nrf2 through a combination of hydrophobic interactions and hydrogen bonding, thereby potentially promoting the activation of the antioxidant Nrf2-Keap1 pathway [58]. This hypothesis is further supported by experimental results from Western blot and qPCR analyses, which show an increase in Nrf2 expression levels following treatment with *C. sativa* extract. A central mechanism underlying the antioxidant activity of flavonoids in SH-SY5Y

cells involves the activation of the Nrf2. Under normal physiological conditions, Nrf2 is sequestered in the cytoplasm by its repressor protein Keap1, which targets it for proteasomal degradation. However, under oxidative stress—such as that modulated by flavonoid treatment—Keap1 undergoes conformational changes or degradation, allowing Nrf2 to dissociate and translocate into the nucleus and binds to antioxidant response elements (ARE) in the DNA, leading to the transcriptional upregulation of phase II detoxification enzymes—such as HO-1, NQO1, glutathione peroxidase, and others (Fig. 11)—which restore redox balance and enhance cellular defence mechanisms [13, 59]. In contrast phenolic acids like caffeoyl or protocatecuic derivates exerted a lower affinity suggesting a moderate role in Nrf2 activation compared to flavonoid compounds.

Activation of Nrf2 not only reduces ROS levels but also impacts mitochondrial integrity and the balance of apoptotic regulators. By modulating the expression of proteins involved in the apoptotic pathway—such as decreasing the pro-apoptotic Bax and increasing anti-apoptotic Bcl-2—Nrf2 contributes to the stabilization of the mitochondrial membrane potential and prevents the release of cytochrome c, a key step in the intrinsic apoptotic cascade [60,61]. The regulation of apoptosis is critically governed by an intricate network involving the tumour suppressor protein p53 and the Bcl-2 family members, particularly Bax and Bcl-2 [62]. Functional p53 ensures cellular homeostasis by enhancing expression and activity of pro-apoptotic Bax while concurrently suppressing anti-apoptotic Bcl-2, thereby setting a threshold for apoptosis. Disruption of this balance—whether through p53 mutations or altered Bax/Bcl-2 ratios—is a hallmark of many cancers and is closely linked to tumour survival and resistance to therapy [63]. When oxidative stress surpasses the adaptative capacity of neuronal cells, p53 triggers a pro-oxidative response that culminates in cell death. Even though the molecular shift governing the polarity of the p53 response remains unclear, it appears to operate through the activation of a distinct subset of OS-responsive genes and signalling pathways. Luteolin acts to scavenge ROS, thereby reducing oxidative damage and the subsequent risk of uncontrolled apoptosis in neuronal cells. This dual functionality allows luteolin not only to induce apoptosis in cancerous cells when desired, but also to provide neuroprotection under conditions of toxin-induced oxidative stress. For instance, in models of MPP^+-induced neurotoxicity, luteolin pre-treatment has been shown to suppress oxidative stress by stabilizing mitochondrial integrity and regulating apoptotic signalling pathways via p53 and the Bax/Bcl-2 axis. Furthermore, the ability of luteolin to modulate intracellular signalling extends to its effects on kinases such as Akt and GSK3β, which contribute to the maintenance of cell survival. By enhancing the phosphorylation of GSK3β and promoting anti-apoptotic signals, luteolin contributes to an environment that, depending on the context, may favour cell survival over apoptosis. [64].

Certain studies have established a crosstalk between the Nrf2 (cytoprotective) and NF-κB (pro-inflammatory) signalling pathways, with evidence that their respective target proteins can reciprocally influence each other's activity [65,66]. NF-κB is a transcription factor that, once activated by oxidative stress or inflammatory stimuli, translocates to the nucleus and initiates transcription of various pro-inflammatory mediators such as TNF-α, IL-1β, and IL-6 [67]. Flavonoids inhibit the activation of NF-κB by preventing the phosphorylation and subsequent degradation of its inhibitory protein, IκB. This suppression leads to reduced transcription of inflammatory genes, including iNOS, thereby creating a synergistic effect with their antioxidative actions [68,69]. In these cells, flavonoids have been shown to mitigate oxidative stress-induced damage by reducing ROS, downregulating NF-κB activation, and inhibiting nitric oxide synthesis [15,70].

Antioxidant treatment may initially decrease oxidative stress in neurons by neutralizing ROS and reducing cellular damage. However, in some cases, this reduction in oxidative stress can lead to a compensatory increase in IL-6 levels as part of the inflammatory response as suggested by Fig. 5B. Although direct evidence for IL-8 suppression in SH-SY5Y

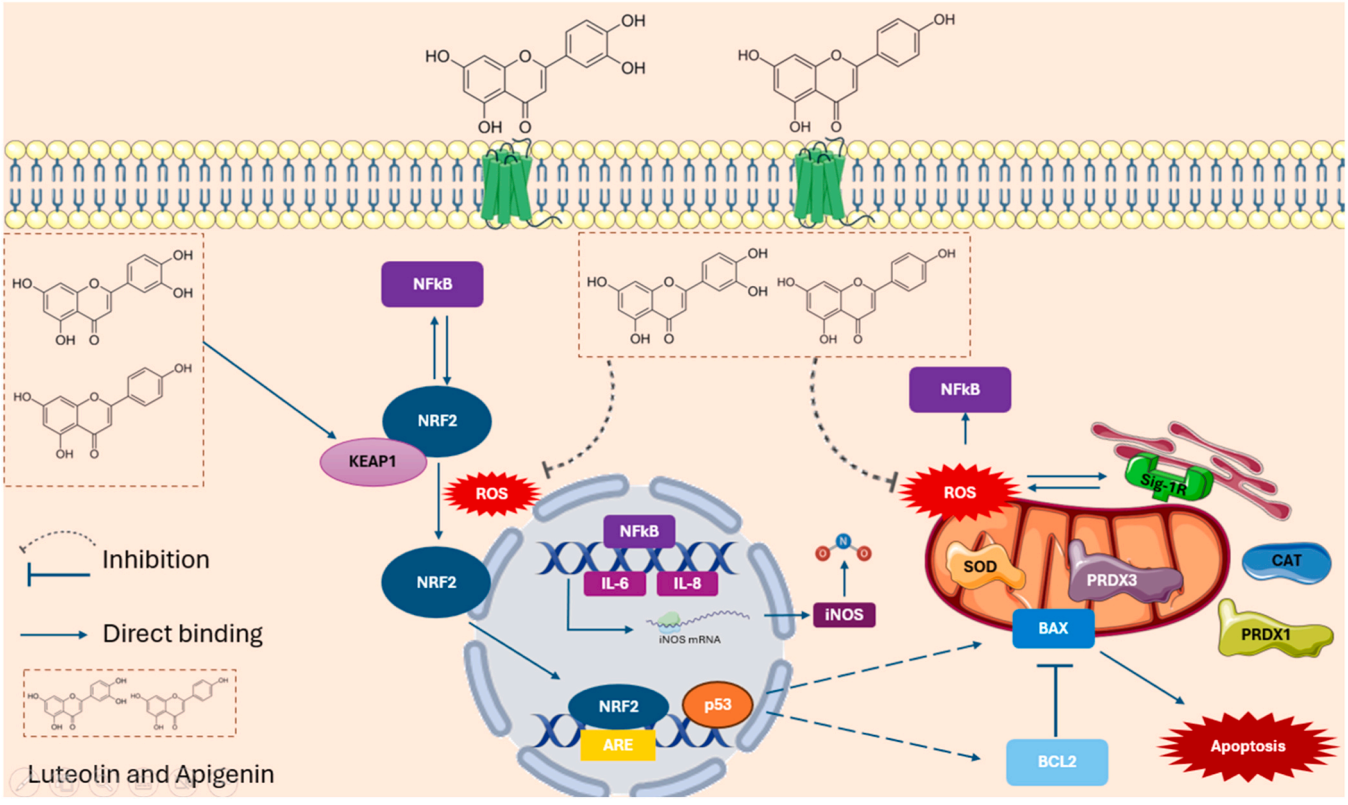

Fig. 11. Schematic representation of potential mechanisms of *Cannabis sativa* polyphenolic fraction in modulating apoptosis and endogenous antioxidant enzymes under oxidative stress.

cells is scarce, the overall anti-inflammatory profile of these flavonoids suggests they may indirectly reduce IL-8 levels by dampening upstream inflammatory signalling [31]. Another critical protein implicated in the development of neuroinflammation is the Sigma-1 receptor (Sigma1R), an endoplasmic reticulum-resident chaperone that functions as a pivotal regulator of cellular homeostasis. Sigma1R plays a central role in modulating oxidative and endoplasmic reticulum stress responses, regulating intracellular calcium signalling, and maintaining mitochondrial integrity and function [30,71].

Importantly, while most observed effects align with well-characterized polyphenol-mediated pathways, the involvement of Sigma-1 receptor signalling points to an additional, less canonical mechanism related to endoplasmic reticulum–mitochondria stress modulation [72]. Although apigenin-7-O-glucuronide also showed a favourable docking score toward Sigma1R, molecular dynamics simulations indicated that stable binding would require a substantial conformational rearrangement of the receptor. Notably, a conformational change was observed during the simulation; however, this rearrangement corresponded to ligand-induced oligomerization and trimer formation rather than to a productive adaptation of the canonical binding pocket [41]. As a result, the active site became structurally inaccessible, precluding stable ligand accommodation under the simulated conditions. It should be noted that the molecular dynamics simulations were necessarily limited in timescale due to the high computational cost associated with the system. While sufficient to capture early conformational responses and assess binding stability trends, the simulation length may not allow for complete conformational equilibration. Consequently, extended simulations on the order of tens to hundreds of nanoseconds will be required in future studies to fully characterize long-timescale receptor dynamics and potential binding modes. Molecular dynamics analyses suggest a lower propensity for stable binding to Sigma1R, as ligand association was not maintained at the binding site under dynamic conditions. The *in silico* results are in agreement with the *in vitro* findings, as the preferential interaction with Nrf2 observed in the docking analysis is consistent with the increased Nrf2 expression detected by Western blot and qPCR following treatment with *C. sativa* extract. Although this pathway was not fully dissected in the present study, it represents an unexpected and potentially relevant component that warrants further mechanistic investigation. Sigma1R activation is closely associated with neuroprotection; for example, its stimulation by established agonists like fluoxetine has been linked to enhanced expression of neurotrophic factors (BDNF) and simultaneous downregulation of inflammatory cytokines such as IL-6 and IL-8 [30,31]. This is the first study to show that polyphenols from *Cannabis sativa* exert its neuroprotective effect through Sigma-1R in SH-SY5Y.

Finally, in the present work, the neuroprotective and redox-modulating effects of the *Cannabis sativa* polyphenolic fraction were characterized in a single human neuroblastoma cell line using an acute oxidative stress paradigm, which inherently limits direct extrapolation to the *in vivo* situation. Future studies in animal models of neurodegeneration and mitochondrial dysfunction will therefore be required to validate the protective effects observed here, to assess pharmacokinetics and bioavailability, and to determine whether standardized polyphenolic formulations can provide benefit in more complex biological contexts.

5. Conclusion

In summary, the phenolic fraction of *Cannabis sativa* L. is critical as it exhibits cytoprotective and antioxidant effects in SH-SY5Y neuroblastoma cells exposed to oxidative stress conditions. According to the results obtained in this manuscript, different concentrations of this aqueous fraction effectively modulate the cellular redox environment via the Keap1/Nrf2 signalling axis, leading to increased expression of antioxidant proteins such as PRDX1, PRDX3, and Nrf2, and enhancing the activity of endogenous antioxidant enzymes.

Moreover, the extract demonstrated neuroprotective activity by preventing apoptosis, as evidenced by modulation of the Bax/Bcl-2 pathway, and significantly attenuated inflammatory responses through the downregulation of NO levels, NF-κB, IL-6, and IL-8. These findings suggest a dual protective mechanism involving both the reduction of endoplasmic reticulum stress-induced apoptosis and the suppression of inflammatory pathways.

In addition, *in silico* molecular docking studies revealed a consistent interaction between phenolic ligands present in *Cannabis sativa* and Leu583 in the Nrf2 protein, highlighting its potential role in stabilizing ligand-protein binding and supporting the *in vitro* data.

Collectively, these results position phenolic compounds present in *Cannabis sativa* as promising and essential key candidates for targeting mitochondrial dysfunction and oxidative neurotoxicity, although further studies are needed to fully the therapeutic and clinical potential. In fact, the use of an unrefined or partially purified Cannabis phenolic fraction has potential translational advantages, including the possibility of synergistic interactions among multiple flavonoids and phenolic acids, lower production complexity relative to single synthetic entities, and alignment with existing hemp-derived products. At the same time, this strategy faces relevant limitations for clinical translation, such as batch-to-batch variability, more complex pharmacokinetics, and regulatory footraces compared with purified polyphenols, so our data are best viewed as proof-of-concept identifying Cannabis phenolics as a source of lead structures and as a basis for standardized, possibly more refined formulations.

CRediT authorship contribution statement

Lucía Ventura: Methodology, Formal analysis, Data curation. **Henar Rojas-Márquez:** Writing – review & editing, Writing – original draft, Methodology, Formal analysis, Data curation, Conceptualization. **Filippo Maggi:** Resources, Project administration, Methodology. **Cristina Moliner:** Methodology, Formal analysis, Data curation. **Guillermo Cásedas:** Writing – review & editing, Writing – original draft, Formal analysis, Data curation, Conceptualization. **Víctor López:** Writing – review & editing, Writing – original draft, Supervision, Methodology, Funding acquisition, Conceptualization. **Ainara Rubio-Castellanos:** Validation, Supervision, Methodology.

Declaration of Competing Interest

The authors declare that they have no known competing financial interests or personal relationships that could have appeared to influence the work reported in this paper.

Acknowledgements

This work was supported by Universidad San Jorge through the calls 2024 and 2025 for internal projects (project ID 2324026 and project ID 2425013). Article Processing Charges are covered by Universidad San Jorge through Convocatoria para la Publicación de Artículos en Acceso Abierto. Cursos 2024-2025 y 2025-2026. We also thank Government of Aragon for the grant received to the Phyto-Pharm group (Ref. B44_23R).

Data availability

Data will be made available on request.

References

[1] A. Salehi, K. Puchalski, Y. Shokoohinia, B. Zolfaghari, S. Asgary, Differentiating Cannabis Products: Drugs, Food, and Supplements, (n.d.). https://doi.org/10.3389/fphar.2022.906038.
[2] F. Pollastro, A. Minassi, L.G. Fresu, Cannabis phenolics and their bioactivities, Curr. Med. Chem. 25 (2017) 1160–1185, https://doi.org/10.2174/0929867324666170810164636.

[3] E. Mazzara, R. Carletti, R. Petrelli, A.M. Mustafa, G. Caprioli, D. Fiorini, S. Scortichini, S. Dall'Acqua, S. Sut, S. Nuñez, V. López, V.D. Zheljazkov, G. Bonacucina, F. Maggi, M. Cespi, Green extraction of hemp (Cannabis sativa L.) using microwave method for recovery of three valuable fractions (essential oil, phenolic compounds and cannabinoids): a central composite design optimization study, J. Sci. Food Agric. (2022), https://doi.org/10.1002/JSFA.11971.
[4] F. Ma, S. Luo, C. Lu, X. Jiang, K. Chen, J. Deng, S. Ma, Z. Li, The role of Nrf2 in periodontal disease by regulating lipid peroxidation, inflammation and apoptosis, Front. Endocrinol. (Lausanne) 13 (2022), https://doi.org/10.3389/fendo.2022.963451.
[5] J. Zhou, F. Chen, A. Yan, X. Xia, Madecassoside protects retinal pigment epithelial cells against hydrogen peroxide-induced oxidative stress and apoptosis through the activation of Nrf2/HO-1 pathway, Biosci. Rep. 40 (2020), https://doi.org/10.1042/BSR20194347.
[6] İ. Gulcin, Antioxidants and antioxidant methods: an updated overview, Arch. Toxicol. 94 (2020) 651–715, https://doi.org/10.1007/s00204-020-02689-3.
[7] S. Kumar, R. Krishna Chaitanya, V.R. Preedy, Assessment of antioxidant potential of dietary components. HIV/AIDS: Oxidative Stress and Dietary Antioxidants, Elsevier, 2017, pp. 239–253, https://doi.org/10.1016/B978-0-12-809853-0.00020-1.
[8] J.B. Owen, D.A. Butterfield, Measurement of oxidized/reduced glutathione ratio, Protein Misfolding Cell. Stress Dis. Aging. Concepts Protoc. Methods Mol. Biol. 648 (2010) 269–277, https://doi.org/10.1007/978-1-60761-756-3_18.
[9] B. Manta, M. Hugo, C. Ortiz, G. Ferrer-Sueta, M. Trujillo, A. Denicola, The peroxidase and peroxynitrite reductase activity of human erythrocyte peroxiredoxin 2, Arch. Biochem. Biophys. 484 (2009) 146–154, https://doi.org/10.1016/j.abb.2008.11.017.
[10] N. Kelsey, W. Hulick, A. Winter, E. Ross, D. Linseman, Neuroprotective effects of anthocyanins on apoptosis induced by mitochondrial oxidative stress, Nutr. Neurosci. 14 (2011) 249–259, https://doi.org/10.1179/1476830511Y.0000000020.
[11] C.P. Ramsey, C.A. Glass, M.B. Montgomery, K.A. Lindl, G.P. Ritson, L.A. Chia, R. L. Hamilton, C.T. Chu, K.L. Jordan-Sciutto, Expression of Nrf2 in neurodegenerative diseases, J. Neuropathol. Exp. Neurol. 66 (2007) 75–85, https://doi.org/10.1097/nen.0b013e31802d6da9.
[12] M. Redza-Dutordoir, D.A. Averill-Bates, Activation of apoptosis signalling pathways by reactive oxygen species, Biochim. et Biophys. Acta (BBA) Mol. Cell Res. 1863 (2016) 2977–2992, https://doi.org/10.1016/j.bbamcr.2016.09.012.
[13] V. Ngo, M.L. Duennwald, Nrf2 and oxidative stress: a general overview of mechanisms and implications in human disease, Antioxidants 11 (2022), https://doi.org/10.3390/antiox11122345.
[14] Y. Chen, E. McMillan-Ward, J. Kong, S.J. Israels, S.B. Gibson, Oxidative stress induces autophagic cell death independent of apoptosis in transformed and cancer cells, Cell Death Differ. 15 (2008) 171–182, https://doi.org/10.1038/sj.cdd.4402233.
[15] S. Devi, V. Kumar, S.K. Singh, A.K. Dubey, J.-J. Kim, Flavonoids: potential candidates for the treatment of neurodegenerative disorders, Biomedicines 9 (2021) 99, https://doi.org/10.3390/biomedicines9020099.
[16] N. Rahman, H. Khan, A. Zia, A. Khan, S. Fakhri, M. Aschner, K. Gul, L. Saso, Bcl-2 modulation in p53 signaling pathway by flavonoids: a potential strategy towards the treatment of cancer, Int. J. Mol. Sci. 22 (2021) 11315, https://doi.org/10.3390/ijms222111315.
[17] A. Kafoud, Z. Salahuddin, R.S. Ibrahim, R. Al-Janahi, A. Mazurakova, P. Kubatka, D. Büsselberg, Potential treatment options for neuroblastoma with polyphenols through anti-proliferative and apoptotic mechanisms, Biomolecules 13 (2023) 563, https://doi.org/10.3390/biom13030563.
[18] C. Lopez-Sanchez, V. Garcia-Martinez, J. Poejo, V. Garcia-Lopez, J. Salazar, C. Gutierrez-Merino, Early reactive A1 astrocytes induction by the Neurotoxin 3-Nitropropionic acid in rat brain, Int. J. Mol. Sci. 21 (2020) 3609, https://doi.org/10.3390/ijms21103609.
[19] X. Chen, Y. Hu, Z. Cao, Q. Liu, Y. Cheng, Cerebrospinal fluid inflammatory cytokine aberrations in Alzheimer's Disease, Parkinson's Disease and amyotrophic lateral sclerosis: a systematic review and meta-analysis, Front. Immunol. 9 (2018), https://doi.org/10.3389/fimmu.2018.02122.
[20] J. Li, Y. Liu, L. Wang, Z. Gu, Z. Huan, H. Fu, Q. Liu, Hesperetin protects SH-SY5Y cells against 6- hydroxydopamine-induced neurotoxicity via activation of NRF2/ARE signaling pathways, Trop. J. Pharm. Res. 19 (2020) 1197–1201, https://doi.org/10.4314/tjpr.v19i6.12.
[21] M. Ikram, T. Muhammad, S.U. Rehman, A. Khan, M.G. Jo, T. Ali, M.O. Kim, Hesperetin confers neuroprotection by regulating Nrf2/TLR4/NF-κB signaling in an Aβ mouse model, Mol. Neurobiol. 56 (2019) 6293–6309, https://doi.org/10.1007/s12035-019-1512-7.
[22] S.H. Jo, M.E. Kim, J.H. Cho, Y. Lee, J. Lee, Y.-D. Park, J.S. Lee, Hesperetin inhibits neuroinflammation on microglia by suppressing inflammatory cytokines and MAPK pathways, Arch. Pharm. Res 42 (2019) 695–703, https://doi.org/10.1007/s12272-019-01174-5.
[23] N. Drewes, X. Fang, N. Gupta, D. Nie, Pharmacological and pathological implications of Sigma-1 receptor in neurodegenerative diseases, Biomedicines 13 (2025) 1409, https://doi.org/10.3390/biomedicines13061409.
[24] T. Siddiqui, L.K. Bhatt, Targeting Sigma-1 receptor: a promising strategy in the treatment of Parkinson's disease, Neurochem. Res 48 (2023) 2925–2935, https://doi.org/10.1007/s11064-023-03960-6.
[25] D. Vauzour, K. Vafeiadou, A. Rodriguez-Mateos, C. Rendeiro, J.P.E. Spencer, The neuroprotective potential of flavonoids: a multiplicity of effects, Genes Nutr. 3 (2008) 115–126, https://doi.org/10.1007/s12263-008-0091-4.
[26] S.J. Maleki, J.F. Crespo, B. Cabanillas, Anti-inflammatory effects of flavonoids, Food Chem. 299 (2019) 125124, https://doi.org/10.1016/j.foodchem.2019.125124.
[27] J.A. Evans, P. Mendonca, K.F.A. Soliman, Neuroprotective effects and therapeutic potential of the citrus flavonoid hesperetin in neurodegenerative diseases, Nutrients 14 (2022) 2228, https://doi.org/10.3390/nu14112228.
[28] Q.Q. Pang, J.H. Kim, H.Y. Kim, J.-H. Kim, E.J. Cho, Protective Effects and Mechanisms of Pectolinarin against H2O2-induced oxidative stress in SH-SY5Y neuronal cells, Molecules 28 (2023) 5826, https://doi.org/10.3390/molecules28155826.
[29] S.L. Costa, V.D.A. Silva, C. dos Santos Souza, C.C. Santos, I. Paris, P. Muñoz, J. Segura-Aguilar, Impact of plant-derived flavonoids on neurodegenerative diseases, Neurotox. Res. 30 (2016) 41–52, https://doi.org/10.1007/s12640-016-9600-1.
[30] M.V. Voronin, E.V. Abramova, E.R. Verbovaya, Y.V. Vakhitova, S.B. Seredenin, Chaperone-dependent mechanisms as a pharmacological target for neuroprotection, Int. J. Mol. Sci. 24 (2023) 823, https://doi.org/10.3390/ijms24010823.
[31] J. Walczak-Nowicka, M. Herbet, Acetylcholinesterase inhibitors in the treatment of neurodegenerative diseases and the role of acetylcholinesterase in their pathogenesis, Int. J. Mol. Sci. 22 (2021) 9290, https://doi.org/10.3390/ijms22179290.
[32] C. Fernández-Moriano, E. González-Burgos, P.K. Divakar, A. Crespo, M.P. Gómez-Serranillos, Evaluation of the antioxidant capacities and cytotoxic effects of Ten Parmeliaceae Lichen species, Evid. Based Complement. Altern. 201 (11) (2016), https://doi.org/10.1155/2016/3169751.
[33] C.P. LeBel, H. Ischiropoulos, S.C. Bondy, Evaluation of the probe 2',7'-dichlorofluorescin as an indicator of reactive oxygen species formation and oxidative stress, Chem. Res. Toxicol. 5 (1992) 227–231, https://doi.org/10.1021/tx00026a012.
[34] L. Schmölz, M. Wallert, S. Lorkowski, Optimized incubation regime for nitric oxide measurements in murine macrophages using the Griess assay, J. Immunol. Methods 449 (2017) 68–70, https://doi.org/10.1016/j.jim.2017.06.012.
[35] DeepMind, AlphaFold Protein Structure Database [Nrf2 - Q16236], (2021). ⟨https://alphafold.com/entry/Q16236⟩ (accessed July 16, 2025).
[36] G.M. Morris, D.S. Goodsell, M.E. Pique, R. Huey, S. Forli, W.E. Hart, S. Halliday, R. Belew, A.J. Olson, User Guide AutoDock Version 4.2 Updated for version 4.2.6 Automated Docking of Flexible Ligands to Flexible Receptors, 1991. ⟨http://autodock.scripps.edu/⟩.
[37] A.A.A. Abdusalam, V. Murugaiyah, Identification of potential inhibitors of 3CL protease of SARS-CoV-2 from ZINC database by molecular docking-based virtual screening, Front. Mol. Biosci. 7 (2020), https://doi.org/10.3389/fmolb.2020.603037.
[38] S. Kim, J. Chen, T. Cheng, A. Gindulyte, J. He, S. He, Q. Li, B.A. Shoemaker, P. A. Thiessen, B. Yu, L. Zaslavsky, J. Zhang, E.E. Bolton, PubChem 2025 update, Nucleic Acids Res. 53 (2025) D1516–D1525, https://doi.org/10.1093/nar/gkae1059.
[39] C. S, S. D.K, V. Ragunathan, P. Tiwari, A. S, P. B.D, Molecular docking, validation, dynamics simulations, and pharmacokinetic prediction of natural compounds against the SARS-CoV-2 main-protease, J. Biomol. Struct. Dyn. 40 (2022) 585–611, https://doi.org/10.1080/07391102.2020.1815584.
[40] H.R. Schmidt, S. Zheng, E. Gurpinar, A. Koehl, A. Manglik, A.C. Kruse, Crystal structure of the human σ1 receptor, Nature 532 (2016) 527–530, https://doi.org/10.1038/nature17391.
[41] M.V. Voronin, Y.V. Vakhitova, I.P. Tsypysheva, D.O. Tsypyshev, I.V. Rybina, R. D. Kurbanov, E.V. Abramova, S.B. Seredenin, Involvement of Chaperone Sigma1R in the anxiolytic effect of Fabomotizole, Int. J. Mol. Sci. 22 (2021) 5455, https://doi.org/10.3390/ijms22115455.
[42] M. Aslam, N. Singh, X. Wang, W. Li, Virtual screening and molecular dynamics simulation to identify inhibitors of the m6A-RNA reader protein YTHDC1, Appl. Sci. 14 (2024) 8391, https://doi.org/10.3390/app14188391.
[43] F. Zare, E. Ataollahi, P. Mardaneh, A. Sakhteman, V. Keshavarz, A. Solhjoo, L. Emami, A combination of virtual screening, molecular dynamics simulation, MM/PBSA, ADMET, and DFT calculations to identify a potential DPP4 inhibitor, Sci. Rep. 14 (2024) 7749, https://doi.org/10.1038/s41598-024-58485-x.
[44] C. Sandoval-Acuña, J. Ferreira, H. Speisky, Polyphenols and mitochondria: an update on their increasingly emerging ROS-scavenging independent actions, Arch. Biochem. Biophys. 559 (2014) 75–90, https://doi.org/10.1016/j.abb.2014.05.017.
[45] B. Bukowska, Current and potential use of biologically active compounds derived from Cannabis sativa L. in the treatment of selected diseases, Int. J. Mol. Sci. 25 (2024) 12738, https://doi.org/10.3390/ijms252312738.
[46] Y. Jin, H. Wang, Naringenin inhibit the hydrogen peroxide-induced SH-SY5Y cells injury through Nrf2/HO-1 pathway, Neurotox. Res. 36 (2019) 796–805, https://doi.org/10.1007/s12640-019-00046-6.
[47] A. Ayna, S.N. Özbolat, E. Darendelioglu, Quercetin, chrysin, caffeic acid and ferulic acid ameliorate cyclophosphamide-induced toxicities in SH-SY5Y cells, Mol. Biol. Rep. 47 (2020) 8535–8543, https://doi.org/10.1007/s11033-020-05896-4.
[48] R. Watanabe, T. Kurose, Y. Morishige, K. Fujimori, Protective effects of Fisetin Against 6-OHDA-induced apoptosis by activation of PI3K-Akt signaling in human neuroblastoma SH-SY5Y cells, Neurochem. Res. 43 (2018) 488–499, https://doi.org/10.1007/s11064-017-2445-z.
[49] J.H. Kim, N.G. Quilantang, H.Y. Kim, S. Lee, E.J. Cho, Attenuation of hydrogen peroxide-induced oxidative stress in SH-SY5Y cells by three flavonoids from Acer okamotoanum, Chem. Pap. 73 (2019) 1135–1144, https://doi.org/10.1007/s11696-018-0664-7.

[50] W. Bors, W. Heller, C. Michel, M. Saran, Flavonoids as antioxidants: determination of radical-scavenging efficiencies, Methods Enzym. 186 (1990) 343–355, https://doi.org/10.1016/0076-6879(90)86128-I.
[51] D. Amić, D. Davidović-Amić, D. Beslo, V. Rastija, B. Lucić, N. Trinajstić, SAR and QSAR of the antioxidant activity of flavonoids., Curr Med Chem 14 (2007) 827–845. ⟨http://www.ncbi.nlm.nih.gov/pubmed/17346166⟩ (accessed May 31, 2018).
[52] N. Mairuae, N. Palachai, P. Noisa, The neuroprotective effects of the combined extract of mulberry fruit and mulberry leaf against hydrogen peroxide-induced cytotoxicity in SH-SY5Y Cells, BMC Complement Med. Ther. 23 (2023) 117, https://doi.org/10.1186/s12906-023-03930-z.
[53] M. Szeliga, Peroxiredoxins in neurodegenerative diseases, Antioxidants 9 (2020) 1203, https://doi.org/10.3390/antiox9121203.
[54] H.-X. Zhou, X. Pang, Electrostatic interactions in protein structure, folding, binding, and condensation, Chem. Rev. 118 (2018) 1691–1741, https://doi.org/10.1021/acs.chemrev.7b00305.
[55] Z. Deng, S. Hassan, M. Rafiq, H. Li, Y. He, Y. Cai, X. Kang, Z. Liu, T. Yan, Pharmacological activity of Eriodictyol: the major natural polyphenolic flavanone, Evid. Based Complement. Altern. Med. 2020 (2020), https://doi.org/10.1155/2020/6681352.
[56] L. Crascì, L. Basile, A. Panico, C. Puglia, F. Bonina, P. Basile, L. Rizza, S. Guccione, Correlating in vitro target-oriented screening and docking: inhibition of matrix metalloproteinases activities by flavonoids, Planta Med. 83 (2017) 901–911, https://doi.org/10.1055/s-0043-104775.
[57] I. Abubakari, L.P. Kwiyukwa, L. Paul, Computational analysis of luteolin, apigenin and their derivatives from Allophylus africanus as potential inhibitors of plasmepsin II a malaria target, BMC Chem. 19 (2025) 196, https://doi.org/10.1186/s13065-025-01527-w.
[58] T. Guan, C. Bian, Z. Ma, In vitro and in silico perspectives on the activation of antioxidant responsive element by citrus-derived flavonoids, Front. Nutr. 10 (2023), https://doi.org/10.3389/fnut.2023.1257172.
[59] Y.J. Kim, E.J. Cho, A.Y. Lee, W.T. Seo, Apigenin ameliorates oxidative stress-induced neuronal apoptosis in SH-SY5Y cells, Microbiol. Biotechnol. Lett. 49 (2021) 138–147, https://doi.org/10.48022/mbl.2009.09006.
[60] R. Ji, F. Jia, X. Chen, Z. Wang, W. Jin, J. Yang, Salidroside Alleviates Oxidative Stress and Apoptosis via AMPK/Nrf2 Pathway in DHT-induced Human Granulosa Cell Line KGN, (2021). https://doi.org/10.21203/rs.3.rs-842159/v1.
[61] J.Y. Jeong, H.-J. Cha, E.O. Choi, C.H. Kim, G.-Y. Kim, Y.H. Yoo, H.-J. Hwang, H. T. Park, H.M. Yoon, Y.H. Choi, Activation of the Nrf2/HO-1 signaling pathway contributes to the protective effects of baicalein against oxidative stress-induced DNA damage and apoptosis in HEI193 Schwann cells, Int. J. Med. Sci. 16 (2019) 145–155, https://doi.org/10.7150/ijms.27005.
[62] A. Basu, The relationship between BcI2, Bax and p53: consequences for cell cycle progression and cell death, Mol. Hum. Reprod. 4 (1998) 1099–1109, https://doi.org/10.1093/molehr/4.12.1099.
[63] M.T. Hemann, S.W. Lowe, The p53-Bcl-2 connection, Cell Death Differ. 13 (2006) 1256–1259, https://doi.org/10.1038/sj.cdd.4401962.
[64] R. Reudhabibadh, T. Binlateh, P. Chonpathompikunlert, N. Nonpanya, P. Prommeenate, P. Chanvorachote, P. Hutamekalin, Suppressing Cdk5 activity by luteolin inhibits MPP+-induced apoptotic of neuroblastoma through Erk/Drp1 and Fak/Akt/GSK3β pathways, Molecules 26 (2021) 1307, https://doi.org/10.3390/molecules26051307.
[65] P.A. Tsuji, K.K. Stephenson, K.L. Wade, H. Liu, J.W. Fahey, Structure-activity analysis of flavonoids: direct and indirect antioxidant, and antiinflammatory potencies and toxicities, Nutr. Cancer 65 (2013) 1014–1025, https://doi.org/10.1080/01635581.2013.809127.
[66] N. Wakabayashi, S.L. Slocum, J.J. Skoko, S. Shin, T.W. Kensler, When NRF2 Talks, Who's Listening? Antioxid. Redox Signal 13 (2010) 1649–1663, https://doi.org/10.1089/ars.2010.3216.
[67] E. Rębas, Role of flavonoids in protecting against neurodegenerative diseases—possible mechanisms of action, Int. J. Mol. Sci. 26 (2025) 4763, https://doi.org/10.3390/ijms26104763.
[68] P. Bellavite, Neuroprotective potentials of flavonoids: experimental studies and mechanisms of action, Antioxidants 12 (2023) 280, https://doi.org/10.3390/antiox12020280.
[69] A. Esteban-Fernández, C. Rendeiro, J.P.E. Spencer, D.G. del Coso, M.D.G. de Llano, B. Bartolomé, M.V. Moreno-Arribas, Neuroprotective effects of selected microbial-derived phenolic metabolites and aroma compounds from wine in human SH-SY5Y neuroblastoma cells and their putative mechanisms of action, Front. Nutr. 4 (2017), https://doi.org/10.3389/fnut.2017.00003.
[70] S. Mani, S. Sekar, S. Chidambaram, M. Sevanan, Naringenin protects against 1-methyl-4-phenylpyridinium- induced neuroinflammation and resulting reactive oxygen species production in SH-SY5Y cell line: an in Vitro model of Parkinson's Disease, Pharmacogn. Mag. 14 (2018) 458, https://doi.org/10.4103/pm.pm_23_18.
[71] K. Eskandari, S.-M. Bélanger, V. Lachance, S. Kourrich, Repurposing Sigma-1 receptor-targeting drugs for therapeutic advances in neurodegenerative disorders, Pharmaceuticals 18 (2025) 700, https://doi.org/10.3390/ph18050700.
[72] B. Amiri, M. Yazdani Tabrizi, M. Naziri, F. Moradi, M. Arzaghi, I. Archin, F. Behaein, A. Bagheri Pour, P. Ghannadikhosh, S. Imanparvar, A. Akhtari Kohneshahri, A. Sanaye Abbasi, N. Zerangian, D. Alijanzadeh, H. Ghayyem, A. Azizinezhad, M. Ahmadpour Youshanlui, M. Poudineh, Neuroprotective effects of flavonoids: endoplasmic reticulum as the target, Front. Neurosci. 18 (2024), https://doi.org/10.3389/fnins.2024.1348151.